

AD-A166 864

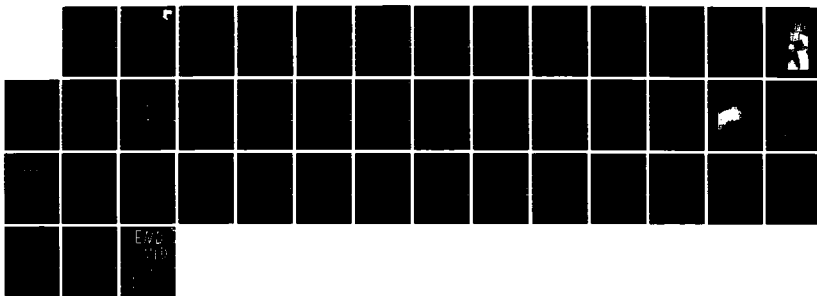
SCANNING PHOTOVOLTAGE TECHNIQUE FOR HIGH RESOLUTION  
NON-DESTRUCTIVE CHARA. (U) ADVANCED RESEARCH AND  
APPLICATIONS CORP SUNNYVALE CA L J PALKUTI ET AL.

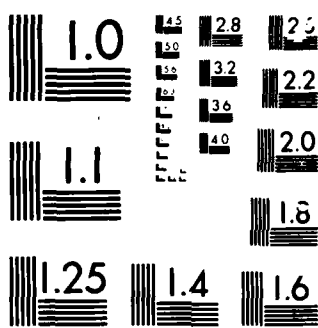
1/1

UNCLASSIFIED

OCT 85 ARACOR-FR-85-351-1 AFMAL-TR-86-4043 F/G 20/12

NL





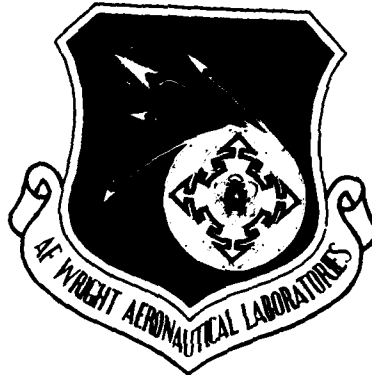
MICROCOPI

CHART

AD-A166 864

AFWAL-TR-86-4043

(2)



SCANNING PHOTOVOLTAGE TECHNIQUE FOR HIGH RESOLUTION  
NON-DESTRUCTIVE CHARACTERIZATION OF SEMICONDUCTOR WAFERS

L.J. Palkuti  
A.A. Milgram  
Advanced Research and Publication Corporation  
Sunnyvale, CA 94086

October 1985

Final Report for Period July 1984 - January 1985

Approved for public release; distribution unlimited.

MATERIALS LABORATORY  
AIR FORCE WRIGHT AERONAUTICAL LABORATORIES  
AIR FORCE SYSTEMS COMMAND  
WRIGHT-PATTERSON AIR FORCE BASE, OHIO 45433-6533

DTIC  
ELECTED  
APR 24 1986  
S E D  
J

FILE COPY

FILE

FILE

0420091

NOTICE

When Government drawings, specifications, or other data are used for any purpose other than in connection with a definitely related Government procurement operation, the United States Government thereby incurs no responsibility nor any obligation whatsoever; and the fact that the government may have formulated, furnished, or in any way supplied the said drawings, specifications, or other data, is not to be regarded by implication or otherwise as in any manner licensing the holder or any other person or corporation, or conveying any rights or permission to manufacture use, or sell any patented invention that may in any way be related thereto.

This report has been reviewed by the Office of Public Affairs (ASD/PA) and is releasable to the National Technical Information Service (NTIS). At NTIS, it will be available to the general public, including foreign nations.

This technical report has been reviewed and is approved for publication.

Dale E Chimenti

DALE E. CHIMENTI  
Nondestructive Evaluation Branch  
Metals and Ceramics Division

FOR THE COMMANDER

M. Forney

D. M. FORNEY, JR., Chief  
Nondestructive Evaluation Branch  
Metals and Ceramics Division

Document for	File
100-1000	<input type="checkbox"/>
100-1001	<input type="checkbox"/>
100-1002	<input type="checkbox"/>
100-1003	<input type="checkbox"/>
100-1004	<input type="checkbox"/>
100-1005	<input type="checkbox"/>
100-1006	<input type="checkbox"/>
100-1007	<input type="checkbox"/>
100-1008	<input type="checkbox"/>
100-1009	<input type="checkbox"/>
100-1010	<input type="checkbox"/>
100-1011	<input type="checkbox"/>
100-1012	<input type="checkbox"/>
100-1013	<input type="checkbox"/>
100-1014	<input type="checkbox"/>
100-1015	<input type="checkbox"/>
100-1016	<input type="checkbox"/>
100-1017	<input type="checkbox"/>
100-1018	<input type="checkbox"/>
100-1019	<input type="checkbox"/>
100-1020	<input type="checkbox"/>
100-1021	<input type="checkbox"/>
100-1022	<input type="checkbox"/>
100-1023	<input type="checkbox"/>
100-1024	<input type="checkbox"/>
100-1025	<input type="checkbox"/>
100-1026	<input type="checkbox"/>
100-1027	<input type="checkbox"/>
100-1028	<input type="checkbox"/>
100-1029	<input type="checkbox"/>
100-1030	<input type="checkbox"/>
100-1031	<input type="checkbox"/>
100-1032	<input type="checkbox"/>
100-1033	<input type="checkbox"/>
100-1034	<input type="checkbox"/>
100-1035	<input type="checkbox"/>
100-1036	<input type="checkbox"/>
100-1037	<input type="checkbox"/>
100-1038	<input type="checkbox"/>
100-1039	<input type="checkbox"/>
100-1040	<input type="checkbox"/>
100-1041	<input type="checkbox"/>
100-1042	<input type="checkbox"/>
100-1043	<input type="checkbox"/>
100-1044	<input type="checkbox"/>
100-1045	<input type="checkbox"/>
100-1046	<input type="checkbox"/>
100-1047	<input type="checkbox"/>
100-1048	<input type="checkbox"/>
100-1049	<input type="checkbox"/>
100-1050	<input type="checkbox"/>
100-1051	<input type="checkbox"/>
100-1052	<input type="checkbox"/>
100-1053	<input type="checkbox"/>
100-1054	<input type="checkbox"/>
100-1055	<input type="checkbox"/>
100-1056	<input type="checkbox"/>
100-1057	<input type="checkbox"/>
100-1058	<input type="checkbox"/>
100-1059	<input type="checkbox"/>
100-1060	<input type="checkbox"/>
100-1061	<input type="checkbox"/>
100-1062	<input type="checkbox"/>
100-1063	<input type="checkbox"/>
100-1064	<input type="checkbox"/>
100-1065	<input type="checkbox"/>
100-1066	<input type="checkbox"/>
100-1067	<input type="checkbox"/>
100-1068	<input type="checkbox"/>
100-1069	<input type="checkbox"/>
100-1070	<input type="checkbox"/>
100-1071	<input type="checkbox"/>
100-1072	<input type="checkbox"/>
100-1073	<input type="checkbox"/>
100-1074	<input type="checkbox"/>
100-1075	<input type="checkbox"/>
100-1076	<input type="checkbox"/>
100-1077	<input type="checkbox"/>
100-1078	<input type="checkbox"/>
100-1079	<input type="checkbox"/>
100-1080	<input type="checkbox"/>
100-1081	<input type="checkbox"/>
100-1082	<input type="checkbox"/>
100-1083	<input type="checkbox"/>
100-1084	<input type="checkbox"/>
100-1085	<input type="checkbox"/>
100-1086	<input type="checkbox"/>
100-1087	<input type="checkbox"/>
100-1088	<input type="checkbox"/>
100-1089	<input type="checkbox"/>
100-1090	<input type="checkbox"/>
100-1091	<input type="checkbox"/>
100-1092	<input type="checkbox"/>
100-1093	<input type="checkbox"/>
100-1094	<input type="checkbox"/>
100-1095	<input type="checkbox"/>
100-1096	<input type="checkbox"/>
100-1097	<input type="checkbox"/>
100-1098	<input type="checkbox"/>
100-1099	<input type="checkbox"/>
100-1100	<input type="checkbox"/>
100-1101	<input type="checkbox"/>
100-1102	<input type="checkbox"/>
100-1103	<input type="checkbox"/>
100-1104	<input type="checkbox"/>
100-1105	<input type="checkbox"/>
100-1106	<input type="checkbox"/>
100-1107	<input type="checkbox"/>
100-1108	<input type="checkbox"/>
100-1109	<input type="checkbox"/>
100-1110	<input type="checkbox"/>
100-1111	<input type="checkbox"/>
100-1112	<input type="checkbox"/>
100-1113	<input type="checkbox"/>
100-1114	<input type="checkbox"/>
100-1115	<input type="checkbox"/>
100-1116	<input type="checkbox"/>
100-1117	<input type="checkbox"/>
100-1118	<input type="checkbox"/>
100-1119	<input type="checkbox"/>
100-1120	<input type="checkbox"/>
100-1121	<input type="checkbox"/>
100-1122	<input type="checkbox"/>
100-1123	<input type="checkbox"/>
100-1124	<input type="checkbox"/>
100-1125	<input type="checkbox"/>
100-1126	<input type="checkbox"/>
100-1127	<input type="checkbox"/>
100-1128	<input type="checkbox"/>
100-1129	<input type="checkbox"/>
100-1130	<input type="checkbox"/>
100-1131	<input type="checkbox"/>
100-1132	<input type="checkbox"/>
100-1133	<input type="checkbox"/>
100-1134	<input type="checkbox"/>
100-1135	<input type="checkbox"/>
100-1136	<input type="checkbox"/>
100-1137	<input type="checkbox"/>
100-1138	<input type="checkbox"/>
100-1139	<input type="checkbox"/>
100-1140	<input type="checkbox"/>
100-1141	<input type="checkbox"/>
100-1142	<input type="checkbox"/>
100-1143	<input type="checkbox"/>
100-1144	<input type="checkbox"/>
100-1145	<input type="checkbox"/>
100-1146	<input type="checkbox"/>
100-1147	<input type="checkbox"/>
100-1148	<input type="checkbox"/>
100-1149	<input type="checkbox"/>
100-1150	<input type="checkbox"/>
100-1151	<input type="checkbox"/>
100-1152	<input type="checkbox"/>
100-1153	<input type="checkbox"/>
100-1154	<input type="checkbox"/>
100-1155	<input type="checkbox"/>
100-1156	<input type="checkbox"/>
100-1157	<input type="checkbox"/>
100-1158	<input type="checkbox"/>
100-1159	<input type="checkbox"/>
100-1160	<input type="checkbox"/>
100-1161	<input type="checkbox"/>
100-1162	<input type="checkbox"/>
100-1163	<input type="checkbox"/>
100-1164	<input type="checkbox"/>
100-1165	<input type="checkbox"/>
100-1166	<input type="checkbox"/>
100-1167	<input type="checkbox"/>
100-1168	<input type="checkbox"/>
100-1169	<input type="checkbox"/>
100-1170	<input type="checkbox"/>
100-1171	<input type="checkbox"/>
100-1172	<input type="checkbox"/>
100-1173	<input type="checkbox"/>
100-1174	<input type="checkbox"/>
100-1175	<input type="checkbox"/>
100-1176	<input type="checkbox"/>
100-1177	<input type="checkbox"/>
100-1178	<input type="checkbox"/>
100-1179	<input type="checkbox"/>
100-1180	<input type="checkbox"/>
100-1181	<input type="checkbox"/>
100-1182	<input type="checkbox"/>
100-1183	<input type="checkbox"/>
100-1184	<input type="checkbox"/>
100-1185	<input type="checkbox"/>
100-1186	<input type="checkbox"/>
100-1187	<input type="checkbox"/>
100-1188	<input type="checkbox"/>
100-1189	<input type="checkbox"/>
100-1190	<input type="checkbox"/>
100-1191	<input type="checkbox"/>
100-1192	<input type="checkbox"/>
100-1193	<input type="checkbox"/>
100-1194	<input type="checkbox"/>
100-1195	<input type="checkbox"/>
100-1196	<input type="checkbox"/>
100-1197	<input type="checkbox"/>
100-1198	<input type="checkbox"/>
100-1199	<input type="checkbox"/>
100-1200	<input type="checkbox"/>
100-1201	<input type="checkbox"/>
100-1202	<input type="checkbox"/>
100-1203	<input type="checkbox"/>
100-1204	<input type="checkbox"/>
100-1205	<input type="checkbox"/>
100-1206	<input type="checkbox"/>
100-1207	<input type="checkbox"/>
100-1208	<input type="checkbox"/>
100-1209	<input type="checkbox"/>
100-1210	<input type="checkbox"/>
100-1211	<input type="checkbox"/>
100-1212	<input type="checkbox"/>
100-1213	<input type="checkbox"/>
100-1214	<input type="checkbox"/>
100-1215	<input type="checkbox"/>
100-1216	<input type="checkbox"/>
100-1217	<input type="checkbox"/>
100-1218	<input type="checkbox"/>
100-1219	<input type="checkbox"/>
100-1220	<input type="checkbox"/>
100-1221	<input type="checkbox"/>
100-1222	<input type="checkbox"/>
100-1223	<input type="checkbox"/>
100-1224	<input type="checkbox"/>
100-1225	<input type="checkbox"/>
100-1226	<input type="checkbox"/>
100-1227	<input type="checkbox"/>
100-1228	<input type="checkbox"/>
100-1229	<input type="checkbox"/>
100-1230	<input type="checkbox"/>
100-1231	<input type="checkbox"/>
100-1232	<input type="checkbox"/>
100-1233	<input type="checkbox"/>
100-1234	<input type="checkbox"/>
100-1235	<input type="checkbox"/>
100-1236	<input type="checkbox"/>
100-1237	<input type="checkbox"/>
100-1238	<input type="checkbox"/>
100-1239	<input type="checkbox"/>
100-1240	<input type="checkbox"/>
100-1241	<input type="checkbox"/>
100-1242	<input type="checkbox"/>
100-1243	<input type="checkbox"/>
100-1244	<input type="checkbox"/>
100-1245	<input type="checkbox"/>
100-1246	<input type="checkbox"/>
100-1247	<input type="checkbox"/>
100-1248	<input type="checkbox"/>
100-1249	<input type="checkbox"/>
100-1250	<input type="checkbox"/>
100-1251	<input type="checkbox"/>
100-1252	<input type="checkbox"/>
100-1253	<input type="checkbox"/>
100-1254	<input type="checkbox"/>
100-1255	<input type="checkbox"/>
100-1256	<input type="checkbox"/>
100-1257	<input type="checkbox"/>
100-1258	<input type="checkbox"/>
100-1259	<input type="checkbox"/>
100-1260	<input type="checkbox"/>
100-1261	<input type="checkbox"/>
100-1262	<input type="checkbox"/>
100-1263	<input type="checkbox"/>
100-1264	<input type="checkbox"/>
100-1265	<input type="checkbox"/>
100-1266	<input type="checkbox"/>
100-1267	<input type="checkbox"/>
100-1268	<input type="checkbox"/>
100-1269	<input type="checkbox"/>
100-1270	<input type="checkbox"/>
100-1271	<input type="checkbox"/>
100-1272	<input type="checkbox"/>
100-1273	<input type="checkbox"/>
100-1274	<input type="checkbox"/>
100-1275	<input type="checkbox"/>
100-1276	<input type="checkbox"/>
100-1277	<input type="checkbox"/>
100-1278	<input type="checkbox"/>
100-1279	<input type="checkbox"/>
100-1280	<input type="checkbox"/>
100-1281	<input type="checkbox"/>
100-1282	<input type="checkbox"/>
100-1283	<input type="checkbox"/>
100-1284	<input type="checkbox"/>
100-1285	<input type="checkbox"/>
100-1286	<input type="checkbox"/>
100-1287	<input type="checkbox"/>
100-1288	<input type="checkbox"/>
100-1289	<input type="checkbox"/>
100-1290	<input type="checkbox"/>
100-1291	<input type="checkbox"/>
100-1292	<input type="checkbox"/>
100-1293	<input type="checkbox"/>
100-1294	<input type="checkbox"/>
100-1295	<input type="checkbox"/>
100-1296	<input type="checkbox"/>
100-1297	<input type="checkbox"/>
100-1298	<input type="checkbox"/>
100-1299	<input type="checkbox"/>
100-1300	<input type="checkbox"/>
100-1301	<input type="checkbox"/>
100-1302	<input type="checkbox"/>
100-1303	<input type="checkbox"/>
100-1304	<input type="checkbox"/>
100-1305	<input type="checkbox"/>
100-1306	<input type="checkbox"/>
100-1307	<input type="checkbox"/>
100-1308	<input type="checkbox"/>
100-1309	<input type="checkbox"/>
100-1310	<input type="checkbox"/>
100-1311	<input type="checkbox"/>
100-1312	<input type="checkbox"/>
100-1313	<input type="checkbox"/>
100-1314	<input type="checkbox"/>
100-1315	<input type="checkbox"/>
100-1316	<input type="checkbox"/>
100-1317	<input type="checkbox"/>
100-1318	<input type="checkbox"/>
100-1319	<input type="checkbox"/>
100-1320	<input type="checkbox"/>
100-1321	<input type="checkbox"/>
100-1322	<input type="checkbox"/>
100-1323	<input type="checkbox"/>
100-1324	<input type="checkbox"/>
100-1325	<input type="checkbox"/>
100-1326	<input type="checkbox"/>
100-1327	<input type="checkbox"/>
100-1328	<input type="checkbox"/>
100-1329	<input type="checkbox"/>
100-1330	<input type="checkbox"/>
100-1331	<input type="checkbox"/>
100-1332	<input type="checkbox"/>
100-1333	<input type="checkbox"/>
100-1334	<input type="checkbox"/>
100-1335	<input type="checkbox"/>
100-1336	<input type="checkbox"/>
100-1337	<input type="checkbox"/>
100-1338	<input type="checkbox"/>
100-1339	<input type="checkbox"/>
100-1340	<input type="checkbox"/>
100-1341	<input type="checkbox"/>
100-1342	<input type="checkbox"/>
100-1343	<input type="checkbox"/>
100-1344	<input type="checkbox"/>
100-1345	<input type="checkbox"/>
100-1346	<input type="checkbox"/>
100-1347	<input type="checkbox"/>
100-1348	<input type="checkbox"/>
100-1349	<input type="checkbox"/>
100-1350	<input type="checkbox"/>
100-1351	<input type="checkbox"/>
100-1352	<input type="checkbox"/>
100-1353	<input type="checkbox"/>
100-1354	<input type="checkbox"/>
100-1355	<input type="checkbox"/>
100-1356	<input type="checkbox"/>
100-1357	<input type="checkbox"/>
100-1358	<input type="checkbox"/>
100-1359	<input type="checkbox"/>
100-1360	<input type="checkbox"/>
100-1361	<input type="checkbox"/>
100-1362	<input type="checkbox"/>
100-1363	<input type="checkbox"/>
100-1364	<input type="checkbox"/>
100-1365	<input type="checkbox"/>
100-1366	<input type="checkbox"/>
100-1367	<input type="checkbox"/>
100-1368	<input type="checkbox"/>
100-1369	<input type="checkbox"/>
100-1370	<input type="checkbox"/>
100-1371	<input type="checkbox"/>
100-1372	<input type="checkbox"/>
100-1373	<input type="checkbox"/>
100-1374	<input type="checkbox"/>
100-1375	<input type="checkbox"/>
100-1376	<input type="checkbox"/>
100-1377	<input type="checkbox"/>
100-1378	<input type="checkbox"/>
100-1379	<input type="checkbox"/>
100-1380	<input type="checkbox"/>
100-1381	<input type="checkbox"/>
100-1382	<input type="checkbox"/>
100-1383	<input type="checkbox"/>
100-1384	<input type="checkbox"/>
100-1385	<input type="checkbox"/>
100-1386	<input type="checkbox"/>
100-1387	<input type="checkbox"/>
100-1388	<input type="checkbox"/>
100-1389	<input type="checkbox"/>
100-1390	<input type="checkbox"/>
100-1391	<input type="checkbox"/>
100-1392	<input type="checkbox"/>
100-1393	<input type="checkbox"/>
100-1394	<input type="checkbox"/>
100-1395	<input type="checkbox"/>
100-1396	<input type="checkbox"/>
100-1397	<input type="checkbox"/>
100-1398	<input type="checkbox"/>
100-1399	<input type="checkbox"/>
100-1400	<input type="checkbox"/>
100-1401	<input type="checkbox"/>
100-1402	<input type="checkbox"/>
100-1403	<input type="checkbox"/>
100-1404	<input type="checkbox"/>
100-1405	<input type="checkbox"/>
100-1406	<input type="checkbox"/>
100-1407	<input type="checkbox"/>
100-1408	<input type="checkbox"/>
100-1409	<input type="checkbox"/>
100-1410	<input type

UNCLASSIFIED

SECURITY CLASSIFICATION OF THIS PAGE

REPORT DOCUMENTATION PAGE

1. REPORT SECURITY CLASSIFICATION Unclassified		1b. RESTRICTIVE MARKINGS										
2. SECURITY CLASSIFICATION AUTHORITY		3. DISTRIBUTION/AVAILABILITY OF REPORT Approved for public release; distribution unlimited.										
4. DECLASSIFICATION/DOWNGRADING SCHEDULE												
PERFORMING ORGANIZATION REPORT NUMBER(S)  FR85-351-1		5. MONITORING ORGANIZATION REPORT NUMBER(S)  AFWAL-TR-86-4043										
6. NAME OF PERFORMING ORGANIZATION Advanced Research and Applications Corp.	6a. OFFICE SYMBOL (if applicable) 7N082	7a. NAME OF MONITORING ORGANIZATION Materials Laboratory (AFWAL/MLLP) A. F. Wright Aeronautical Labs										
7. ADDRESS (City, State, and ZIP Code) 223 E. Arques Ave. unnyvale, CA 94086	7b. ADDRESS (City, State, and ZIP Code) Wright-Patterson AFB, OH 45433											
8. NAME OF FUNDING/SPONSORING ORGANIZATION DCASR - Los Angeles	8b. OFFICE SYMBOL (if applicable) S0506A	9. PROCUREMENT INSTRUMENT IDENTIFICATION NUMBER F33615-84-C-5088										
10. ADDRESS (City, State, and ZIP Code) P. O. Box 45011 Los Angeles, CA 90045	10. SOURCE OF FUNDING NUMBERS <table border="1"><tr><td>PROGRAM ELEMENT NO. 65502F</td><td>PROJECT NO. 3005</td><td>TASK NO. 50</td><td>WORK UNIT ACCESSION NO. 20</td></tr></table>			PROGRAM ELEMENT NO. 65502F	PROJECT NO. 3005	TASK NO. 50	WORK UNIT ACCESSION NO. 20					
PROGRAM ELEMENT NO. 65502F	PROJECT NO. 3005	TASK NO. 50	WORK UNIT ACCESSION NO. 20									
11. TITLE (Include Security Classification) Scanning Photovoltage Technique for High Resolution Non-Destructive Characterization of Semiconductor Wafers												
12. PERSONAL AUTHOR(S) L. J. Palkuti and A. A. Milgram												
a. TYPE OF REPORT Final	13b. TIME COVERED FROM 7/2/84 TO 1/2/85	14. DATE OF REPORT (Year, Month, Day) October 1985	15. PAGE COUNT 43									
16. SUPPLEMENTARY NOTATION												
17. COSATI CODES <table border="1"><tr><th>FIELD</th><th>GROUP</th><th>SUB-GROUP</th></tr><tr><td>20</td><td>12</td><td></td></tr><tr><td></td><td></td><td></td></tr></table>		FIELD	GROUP	SUB-GROUP	20	12					18. SUBJECT TERMS (Continue on reverse if necessary and identify by block number) GaAs photovoltaic non-destructive evaluation defects	
FIELD	GROUP	SUB-GROUP										
20	12											
19. ABSTRACT (Continue on reverse if necessary and identify by block number) <p>Near-surface defects in semiconductor wafers have a primary influence upon device properties, both the yield and radiation hardness. In phase I of this program, a scanning photovoltage (SPV) technique was experimentally evaluated for the high-resolution, non-destructive identification and mapping of near-surface defects in wafers. The SPV technique shows promise of being useful for this purpose in semi-insulating materials such as GaAs, silicon-on-sapphire and InP. All the goals in the Phase I program were met; experimental apparatus was developed and the differential SPV signal correlated with surface dislocation networks in GaAs wafers. The results strongly support the development and further evaluation of the SPV technique.</p> <p>The apparatus utilizes an Ar-ion scanning laser system with a programmable x-y table and a focussed laser beam. A photovoltage signal is measured due to the modulated laser beam.</p>												
20. DISTRIBUTION/AVAILABILITY OF ABSTRACT <input type="checkbox"/> UNCLASSIFIED/UNLIMITED <input checked="" type="checkbox"/> SAME AS RPT. <input type="checkbox"/> DODIC USERS		21. ABSTRACT SECURITY CLASSIFICATION Unclassified										
22a. NAME OF RESPONSIBLE INDIVIDUAL D. E. Chimenti		22b. TELEPHONE (Include Area Code) 513-255-5309	22c. OFFICE SYMBOL AFWAL/MILP									

## TABLE OF CONTENTS

	<u>Page</u>
1.0 INTRODUCTION.....	1
1.1 Significance of the Problem.....	1
1.2 Background of SPV Technique and Applications.....	3
2.0 PROGRAM OBJECTIVES.....	4
3.0 OVERVIEW OF PROGRESS.....	4
4.0 HIGH-RESOLUTION SPV SYSTEM.....	5
4.1 Description of Setup.....	5
4.2 Contact Evaluation.....	10
4.3 Multiple Wavelength Approach.....	10
5.0 EVALUATION OF SPV DEFECT MAPPING.....	13
5.1 Demonstration of Wafer Scan Capability.....	13
5.2 Resolution Measurement.....	16
5.2.1 Scribe-Induced Damage.....	16
5.2.2 Effect of Orientation of Damage Traces.....	22
5.3 GaAs - Effect of Non-Contact Polishing (NCP).....	27
5.4 SOS Films.....	27
6.0 SUMMARY AND CONCLUSIONS.....	34
7.0 RECOMMENDATIONS FOR FUTURE WORK.....	35
8.0 REFERENCES.....	36

## LIST OF FIGURES

<u>Figure</u>	<u>Caption</u>	<u>Page</u>
1	Photograph of Automated Scanning Photovoltage System.....	6
2	Schematic of Original Photovoltage System.....	8
3	Schematic of Photovoltage System with Enhancements Added During Phase I.....	9
4	PV Profiles - As-Received GaAs Wafer.....	11
	A. Sintered Contacts	
	B. Non-Sintered Contacts	
5	PV Profiles as a Function of Position on the Wafer Positions 1 - 9 Shown in Inset.....	14
	A. As-Received GaAs	
	B. NCP GaAs	
6	PV High-Resolution Profiles - As-Received GaAs Wafer.....	15
	A. Area A of Figure 19 Showing Large Signal	
	B. Area B of Figure 19 Showing Small Signal	
7	PV Profile of Scribe Damage on NCP GaAs Wafer.....	18
8	TEM Cross-Section of Scribe Damage - NCP GaAs Wafer.....	19
9	Scribe-Induced Damage.....	20
	A. Schematic	
	B. Micrograph	
10	Scribe-Induced Damage - Lateral Spreading of Defects.....	21
	A. As-Received GaAs	
	B. NCP GaAs	
11	PV High-Resolution Profile Revealing Electrically Active Defects Introduced by Scribing.....	23
	A. As-Received GaAs Wafer	
	B. NCP GaAs Wafer	
12	PV High-Resolution Profiles Along Scribe - As-Received GaAs...	24

LIST OF FIGURES (Continued)

<u>Figure</u>	<u>Caption</u>	<u>Page</u>
13	PV High-Resolution Profiles for Different Scribe Forces - As-Received GaAs Wafer.....	25
14	PV Profiles From SOS Film.....	26
	A. Scan Perpendicular to Lineated Damage	
	B. Scan Parallel to Lineated Damage	
15	PV Profile - As-Received GaAs Wafer.....	28
16	PV High-Resolution Profile - As-Received GaAs Wafer.....	29
17	PV Profile After NCP Processing.....	30
18	PV Profile from SOS Film - Kyocera Sapphire.....	31
19	PV Profile from SOS Film - Union Carbide Sapphire.....	32
20	PV Profile from SOS Film Using Fast Scan-Union Carbide Sapphire.....	33

# SCANNING PHOTOVOLTAGE TECHNIQUE FOR HIGH RESOLUTION NON-DESTRUCTIVE CHARACTERIZATION OF SEMICONDUCTOR WAFERS

## 1.0 INTRODUCTION

### 1.1 Significance of the Problem

All semiconductor technologies would benefit greatly from a high-resolution, simple and inexpensive non-destructive evaluation technique that could characterize the types of defects near a semiconductor surface and map their density and location across a wafer. Near-surface defects have been shown to have an adverse effect on device yield, performance and radiation hardness. In particular, the GaAs industry that fabricates both digital and microwave integrated circuits requires defect mapping because of the proven difficulty in obtaining wafer surfaces that are free of microstructural, sawing and polishing defects, and mounting evidence of the adverse influence of such defects on device performance and yield.

There is, at present, no satisfactory technique for the non-destructive identification and mapping of near-surface defects in semiconductor wafers. Such a capability would be invaluable for wafer selection and device physics applications in support of the development and processing of advanced electronic devices. For example, the Wright Patterson Materials Laboratory is in the process of initiating a four-year MM&T program to develop improved GaAs microwave integrated circuits. This program requires a capability for selecting good wafers or relatively defect-free zones on a wafer.

Many techniques exist for the characterization of semiconductors. Some of these techniques, such as transmission electron microscopy (TEM), are indeed high-resolution techniques, but have inherent disadvantages associated with them. In the case of TEM those disadvantages are:

- (1) The technique is destructive of the material (thin foils of 1000 Å thickness or less have to be prepared).
- (2) The technique is not applicable to the mapping of an entire wafer.

Another technique which is often used is that of defect etching in collaboration with optical microscopy. In this case, whole wafer mapping is a possibility, but again the technique is destructive. Often, many microns of material are etched away in the process of forming visible pits at defects.

Other techniques which have some value for whole-wafer defect characterization of semiconductors include x-ray topography, Rutherford backscattering (RBS) and the electron-beam-induced-conductivity (EBIC) mode of SEM. X-ray topography can be performed using synchrotron radiation or conventional high-intensity x-ray sources in both reflection and transmission geometries. While being quite useful, these techniques offer rather limited defect resolution (probably  $\sim 100 \mu\text{m}$ , depending somewhat on the defect in question) and require either considerable capital investment (x-ray equipment, etc.) or access to synchrotron radiation. Such techniques are, therefore, not generally available to the GaAs industry.

The principal advantage of the Rutherford backscattering (RBS) technique is that it does detect crystalline disorder, whereas the disadvantages are that it is slow, expensive and can lead to further damage of the crystal through radiation damage. The resolution is currently limited to about  $500 \mu\text{m}$ . In addition, effects from stress produced during sample mounting can lead to problems with defect interpretation.

The EBIC mode of SEM, while clearly having a mapping capability and, for defects which can be imaged, an adequate resolution ( $\sim 1 \mu\text{m}$ ), has a sensitivity (signal/noise) that is inadequate to yield useful information regarding near-surface defects in semiconductors. This may be due to the long absorption length of high-energy electrons in semiconductors (a factor of five longer than for the scanning photovoltage technique proposed herein). The EBIC technique does contaminate examined samples, in addition to causing permanent radiation damage. Lastly, it should be pointed out that the technique carries a high degree of "empty" resolution. The typical resolution of 1 micron is several orders of magnitude greater than both the SEM spot size ( $\sim 50 \text{ \AA}$ ), and the wavelength of the incident radiation ( $\sim 0.1 \text{ \AA}$  for 20-keV electrons). This is because of the "pear-shaped" distribution of the energy dissipation of the

incident beam in the semiconductor. In a typical case, a 50-Å-diameter incident beam leads to a 1- $\mu\text{m}$ -sized region of induced current. This phenomenon, together with some applications of EBIC in semiconductors, are discussed by Leamy et al.(1)

Non-destructive optical techniques have also been recently developed that can measure local resistivity variations (dark-spot scanning technique) or variation in local light scattering (for near-surface defect detection and particle counting) in GaAs wafers. The principal advantage of these methods is that they can be used for whole wafer mapping, whereas the disadvantages are that these techniques have poor spatial resolution, are slow and require expensive equipment. Furthermore, the correlation between wafer maps and electrically-active material defects has not been quantitatively established.

## 1.2 Background of SPV Technique and Applications

A high-resolution, non-destructive characterization technique for electrically-active defect mapping on semiconductor wafers that is particularly suitable for defect characterization in semi-insulating GaAs wafers is the scanning photovoltage (SPV) technique. In this method, a highly focussed laser spot is scanned over the sample utilizing a precision x-y stage. The differential photovoltage signal produced between two contacts at the edge of the wafer is proportional to the electrically-active defects encountered by the laser scan. By processing this photovoltage signal, a map of the electrically-active bulk and surface defects can be generated.

The scanning photovoltage (SPV) technique has been utilized in a variety of forms since at least 1959. The first reported use of it was by Oroshnik and Many.(2) They found that resistivity inhomogeneities in germanium constitute small junctions giving rise to easily detectable photovoltages of the order of hundreds of microvolts. They utilized this fact to develop a sensitive and rapid tool for exploring the homogeneity of single-crystal germanium wafers. They used both a differential and an integral version of the technique.

More recently, a group at RCA(3,4,5) have applied both a photovoltage spectroscopy and a laser scanning photovoltage technique in the characterization of silicon-on-sapphire (SOS) material. Using the laser scanning technique,<sup>(4)</sup> they were able to demonstrate that hydrogenation of SOS decreases the magnitude of microscopic inhomogeneities. They have also used this technique<sup>(5)</sup> in both differential and integral (MIS) configurations to show that a high density of microscopic inhomogeneities corresponds to a high density of crystallographic defects such as dislocations and twins, determined using U.V. reflectance and x-ray topography techniques.

Another application reported recently by Chappell, et al.,<sup>(6)</sup> involves the use of surface photovoltage measurements to determine the width of the oxygen precipitate-free zone at the surface of Czochralski-grown silicon wafers.

## 2.0 PROGRAM OBJECTIVES

- Demonstrate a high-resolution SPV technique for semi-insulating GaAs
- Correlate SPV signal with GaAs surface defects
- Investigate use of non-sintered contacts on GaAs wafers
- Consider multiple wavelength PV techniques and automated data handling

## 3.0 OVERVIEW OF PROGRESS

Phase I established the feasibility of a high-resolution photovoltage line-scan technology that can produce subsurface defect maps on GaAs wafers. The results obtained are summarized below:

- A suitable scanning photovoltage system was developed and evaluated for the mapping of subsurface GaAs defects.
- The laser beam spot size was measured, demonstrating a beam diameter of 1.5 microns. Utilizing a 0.5-micron-resolution x-y stage, measurements of minimum size damage traces indicated that 2.5-micron surface dislocation networks of isolated spatial extent could clearly be resolved.

- The SPV line scans were correlated with subsurface damage directly observed with cross-section transmission electron microscopy (XTEM).
- The SPV signal levels correlated directly with the magnitude of damage introduced by controlled diamond scribing.
- Non-sintered contacts, located at the edge of GaAs wafers, were evaluated and compared with alloyed ohmic contacts. Similar SPV scans were produced with sintered ohmic contacts as were obtained with illuminated pressure contacts.
- A full-wafer SPV scan capability was demonstrated and the subsurface damage pattern in GaAs was characterized. After the subsurface damage was removed by an etching process, the differential SPV signal variations were significantly reduced.
- Multisource operation was studied to reduce the effect of spurious signals and reduce the integration times. The SPV aperture was modified to accept other light sources and the use of a dc bias light was investigated. Improvement in the speed to acquire the data and some reduction in the spurious signals from the contact area was demonstrated.

The Phase I program has demonstrated that the SPV method has potential as a high-resolution NDE technique for the quantitative mapping of GaAs subsurface damage. A whole-wafer NDE technique has been demonstrated that indicates that SPV responses can be used to study substrate defects in GaAs. Thus, an SPV instrument would have valuable application for device physics studies or as a Q/A tool.

#### **4.0 HIGH RESOLUTION SPV SYSTEM**

##### **4.1 Description of Set-Up**

The experimental configuration shown in Figure 1 was used to produce high-resolution (near one micron) scanning photovoltage (SPV) responses in GaAs

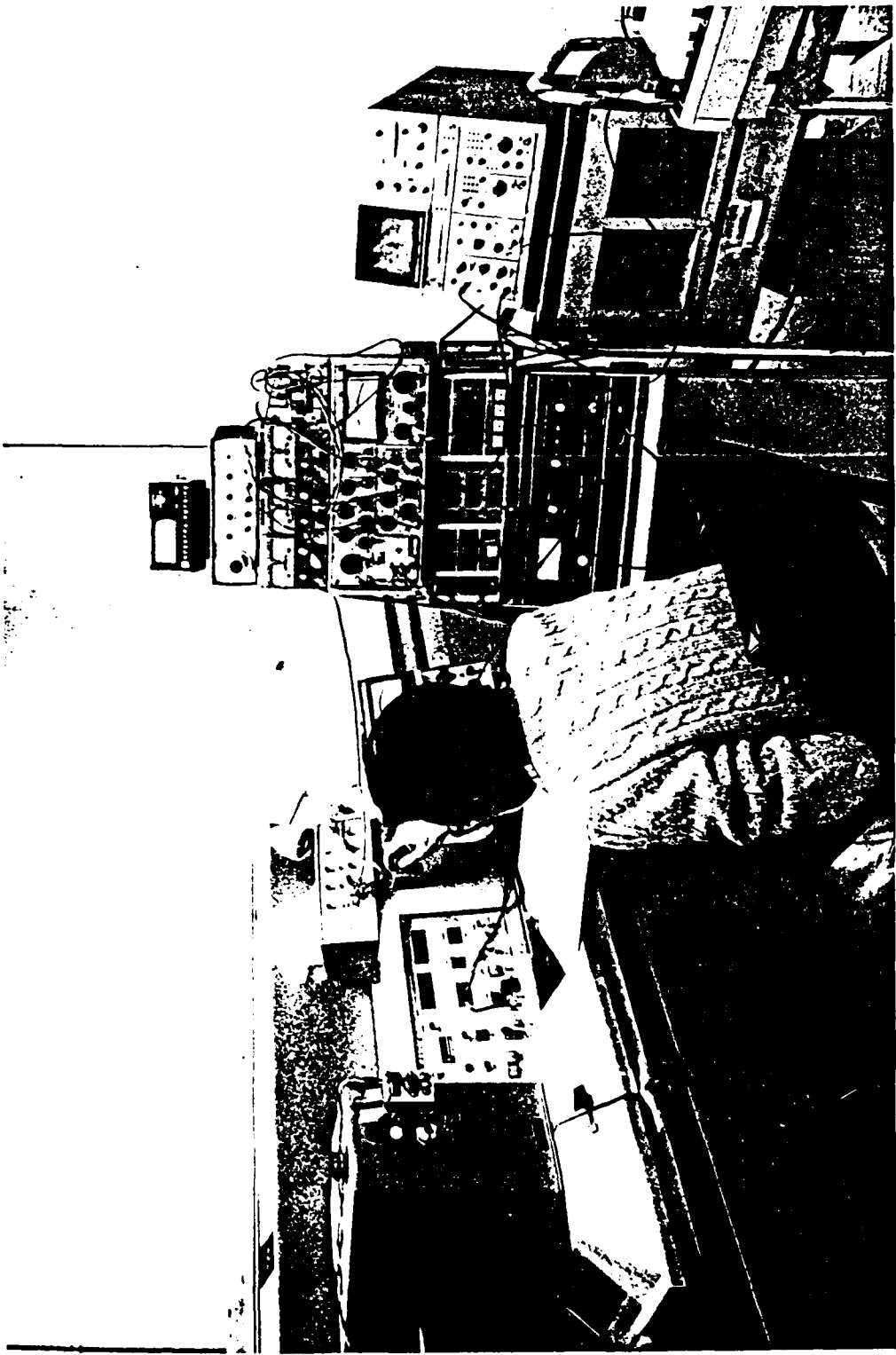


Figure 1. Photograph of Automated Scanning Photovoltage System.

wafers. The block diagram in Figure 2 shows a schematic of the original set-up. Figure 3 shows the inclusion of auto-focus, multiple-wavelength capability and illuminated contacts. An infinity-corrected optical path was implemented incorporating an ultra-long working distance objective (50X, N.A. = 0.55). The argon laser beam ( $\lambda = 518$  nm) is expanded and then focussed to a diffraction-limited spot (calc.  $\sim 1.2$  micron). Since GaAs wafers are not flat and have taper (nominally 10 microns) and dust particles on the chuck also introduce nonflatness, an autofocus system was required to automatically scan large wafers. For direct sample inspection, alignment beam viewing optics were also incorporated. A path to add an additional light source, either for sample illumination and/or for multi-beam applications, was provided.

Wafer translation is provided by a two-level x-y stage that incorporates an electrically-controlled air-bearing stage that can be translated to four inches. High-resolution scanning is provided by a piezoelectric x-y stage with a resolution of 0.5 microns. A digital controller is used to coordinate the motion of these two x-y stages; the resolution of the x-y stage decoder was verified by direct optical observations.

To evaluate the resolution of the SPV system, laser spot-size measurements were conducted by (1) projecting the image of the spot with a long working distance (15 feet) lens; (2) direct photography; (3) by producing a melt spot in a thin (0.5 micron) film of silicon on sapphire substrate; and (4) by detecting the light transmitted through a grating (photomask with one-micron lines and spaces). The best overall estimate of the laser spot size obtained from these measurements is  $1/e$  diameter of  $1.5 \pm 0.1$  microns. This spot size is slightly larger than the expected diffraction limit and can be improved by introducing spatial filtering.

To conduct SPV defect measurements, the wafer was placed on the table and the photovoltage monitored via contacts on the edges of the wafer. The laser beam was modulated internally at 15 Hz, and at a later stage was mechanically chopped. A modulated photovoltage was generated by the modulated laser beam. In this manner, the desired photovoltage signal could be filtered from the noise

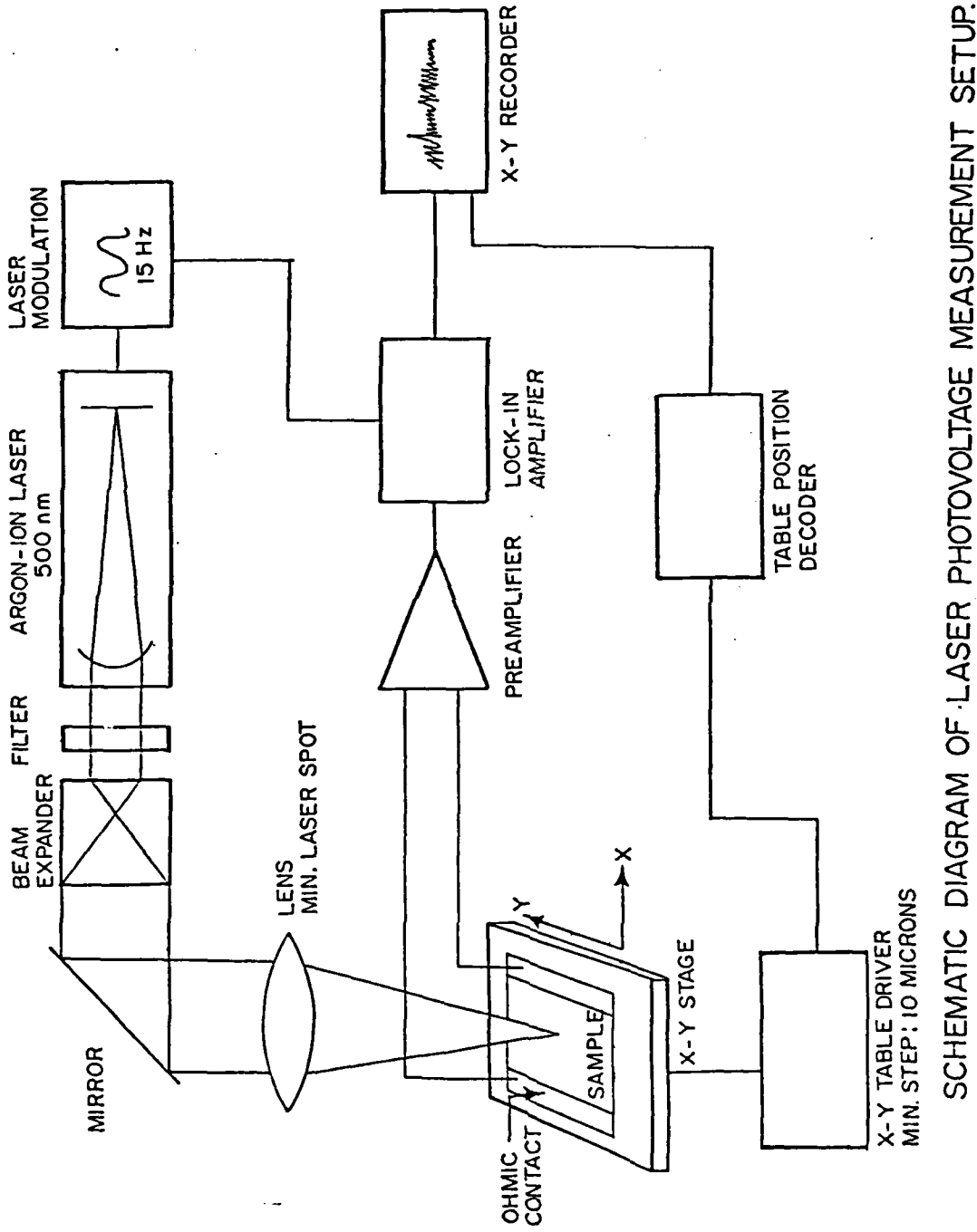


Figure 2. Schematic Diagram of Original Photovoltage Measurement Set.  
SCHEMATIC DIAGRAM OF LASER PHOTOVOLTAGE MEASUREMENT SETUP.

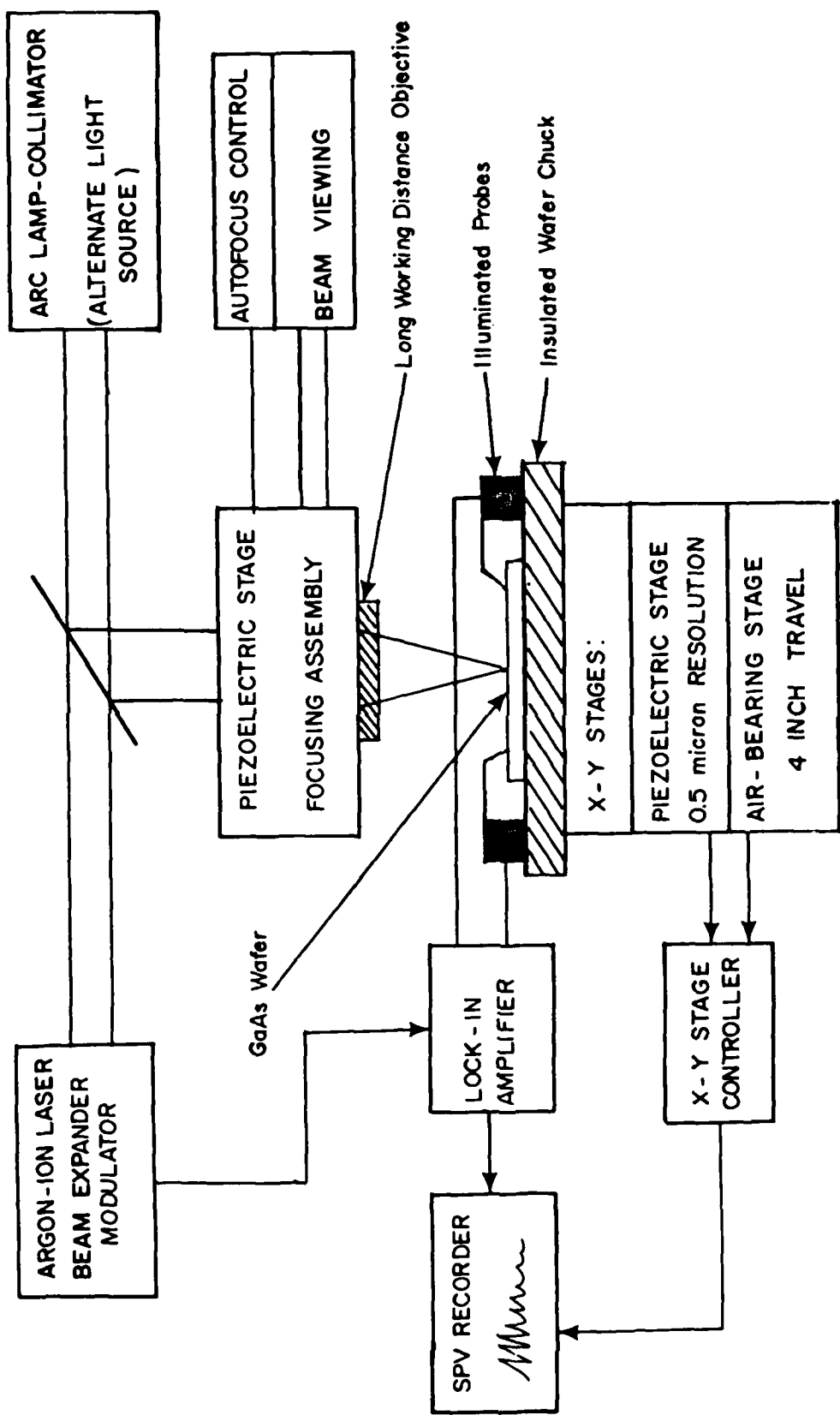


Figure 3. Schematic of Photovoltage System with Enhancements Added During Phase I.

by the use of a sensitive lock-in amplifier and then displayed on the CRT and x-y recorder. Separate "off-line" recording enables spatial profiles of electrically-active defects of the entire wafer to be recorded. We have PV-profiled typical VHSIC SOS films with ultra-violet reflectance (UVR)  $\approx 0$  and have observed extreme lateral variations in the PV response. Typically, the lateral variation has a periodicity of about 40-to-50  $\mu\text{m}$ .

#### 4.2 Contact Evaluation

In previous work, alloyed (sintered) In contacts were utilized to obtain the SPV responses. This is undesirable because alloying the contact is destructive to the sample. In this program, we evaluated a variety of contacts and probes with the objective of eliminating the need for alloying contacts. In this way, potential damage to the wafer by contacting can be minimized. The results of this study indicated that essentially ohmic behavior could be obtained utilizing illuminated indium pressure contacts. These non-sintered contacts were evaluated to determine the effects on the SPV responses. In Figure 4, we show the SPV responses obtained on the same wafer with a set of sintered and illuminated pressure (non-sintered) contacts. These results show essentially identical responses. This result was repeated in a number of separate samples and found to be consistent.

To produce illuminated pressure contacts, we are evaluating a fiber-optic light source combined with microprobes to produce a convenient means of localizing the illumination on the contacts. This approach has produced excellent electrical results, but requires some additional work to obtain acceptable mechanical stability.

#### 4.3 Multiple-Wavelength Techniques

In the SPV technique discussed previously, monochromatic light from an argon-ion laser is modulated and then scanned across a semi-insulating semiconductor sample. A differential photovoltage signal is generated by the light and is detected by a lock-in amplifier. The photovoltage signal results from the interaction of the light with spatial non-uniformities and electrically-active defects in the sample. However, spurious signals, due to scattered light

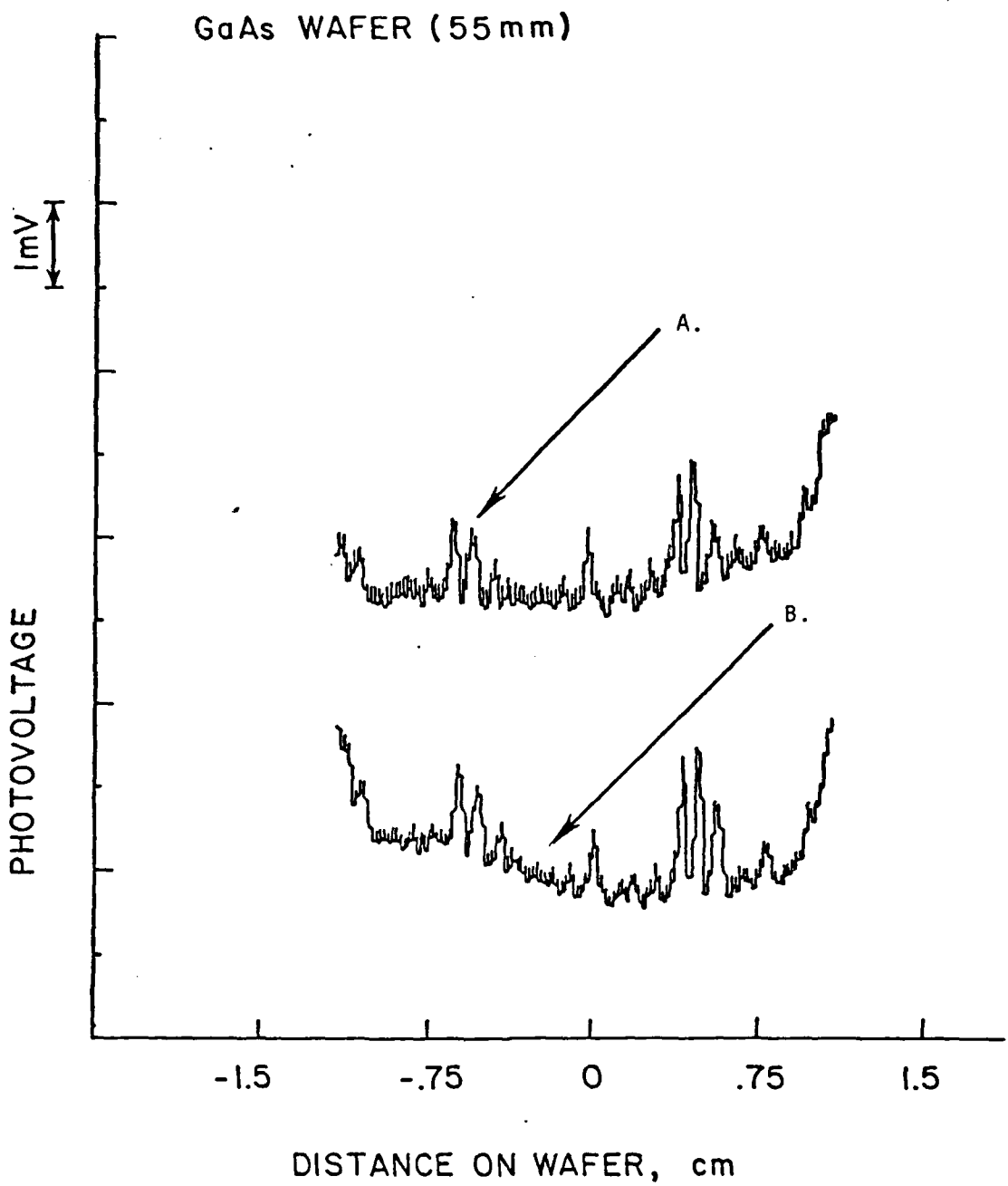


Figure 4. PV Profiles - As-Received GaAs Wafer.  
(A) Sintered Contacts; (B) Non-Sintered Contacts

impinging on the sample contacts, resistivity variations in the sample, barriers introduced at film-semiconductor interfaces and bulk defects, can be a significant part of the experimentally-observed photovoltage signal. In addition, the time constant of the SPV signal can be long due to the high resistance of the sample, which requires a longer time for data collection.

In order to eliminate the spurious components from the photovoltage signal, subtraction techniques using multiple optical sources were investigated. In the first method, an unmodulated light source was used to lower the sample resistivity and consequently decrease the time constant. A second approach was to use another modulated light operating at a different wavelength from the primary beam. In this latter case, spurious components can be eliminated by subtraction techniques. To implement these multi-beam approaches, additional light ports were added to the prototype optical system. These additional ports are indicated as "alternate light source" in the schematic in Figure 3.

A number of alternate light sources were considered during the course of this program. These included a monochromatic laser source, as well as filtered arc-lamp sources. The results of the studies suggested that an optimally filtered arc lamp could provide a suitable source to eliminate both spurious signals and also the signal originating from bulk defects. The measurements with a steady-state bias source showed that the SPV time constants for semi-insulating GaAs samples could be reduced by at least an order of magnitude. Reproducible SPV responses at a modulating frequency of 20-to-50 Hz, were obtained using this method. In addition, the bias source also reduced the spurious signals near the contact areas. Utilizing this bias-light technique, acceptable SPV signals were obtained to within 5 mm of the contact area.

These initial experiments verified the benefits that could be obtained from employing the multi-source SPV method, e.g.: (a) a reduction in effects from spurious signals (i.e., contact effects) and, (b) a reduction in the measurement times. Future work is required to optimize the wavelength of the bias light source and to incorporate modulation in such a way that subtraction techniques can be utilized. These approaches can then be utilized to separate bulk sample inhomogeneities from surface defects.

## 5.0 EVALUATION OF SPV DEFECT MAPPING

### 5.1 Demonstration of Wafer Scan Capability

Figure 5 shows representative SPV profiles obtained over a 30-mm diameter region of a 55-mm (2-inch) LEC-GaAs wafer (as received). These maps were obtained at a scan rate of 0.3 mm/sec or about two minutes per line scan. Immediately apparent is the pattern lineation in the photovoltage signals or the correspondence of many photovoltaic extrema, indicating that polishing and/or handling scratches are the origins of these photovoltaic variations. Also apparent are the variations observed as a function of separation distance,  $\Delta y$ . Scans made on this and similar samples produced a wide variation in the photovoltaic response as a function of position on the wafer surface. For example, area A and area B indicated in Figure 5 show high and low photovoltaic response, respectively. These areas on the wafer are highlighted in Figure 6, where high-resolution scans are given. In Figure 6, line scans are given with 12-micron step size, while the insets show scans at the highest resolution available (here the resolution is limited by the beam spot size to 1.5 microns).

These data show that the surface damage in this wafer has a spatial distribution with peak separations on the order of about 50 microns. This lined damage structure has been observed previously in GaAs and other semiconductors, and is characteristic of damage introduced by incomplete chemi-mechanical polishing. In addition, the high-resolution scans indicate the presence of additional localized damage (see inset) with a  $\leq 10$  micron spatial extent.

The pattern of photovoltaic peak heights shown in Figures 5 and 6 suggest that high-resolution SPV mapping can provide a quantitative measure of substrate damage. In particular, areas of high damage on the wafer are clearly indicated. Note the high signal activity located in the region near the wafer flat. In addition, the largest signal variations and most erratic spatial responses are particularly evident as the edge of the wafer is approached. These characteristic features are also indicative of remnant surface defects.

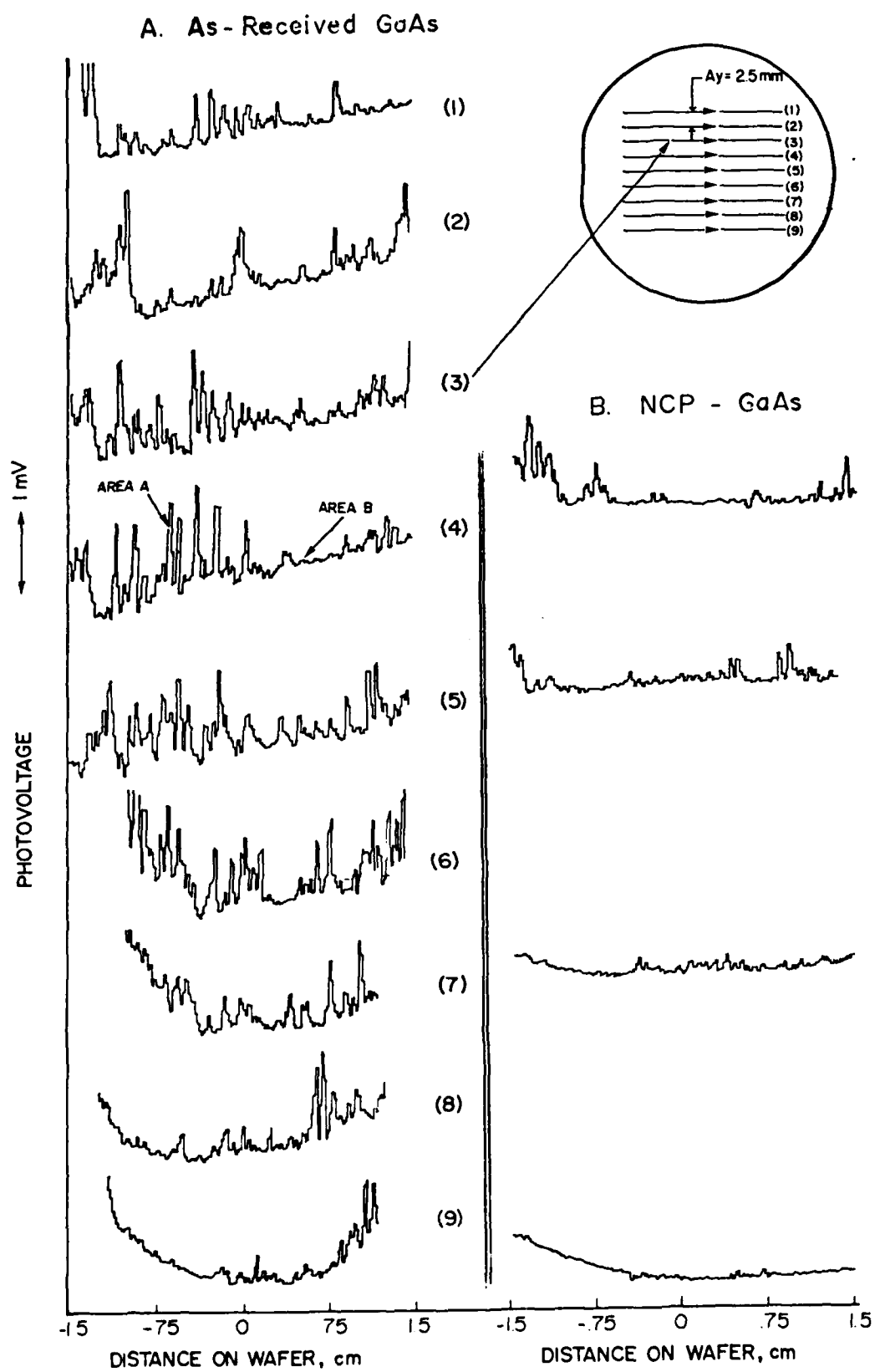


Figure 5. PV Profiles as a Function of Position on the Wafer.  
Positions 1-9 Shown in the Inset.

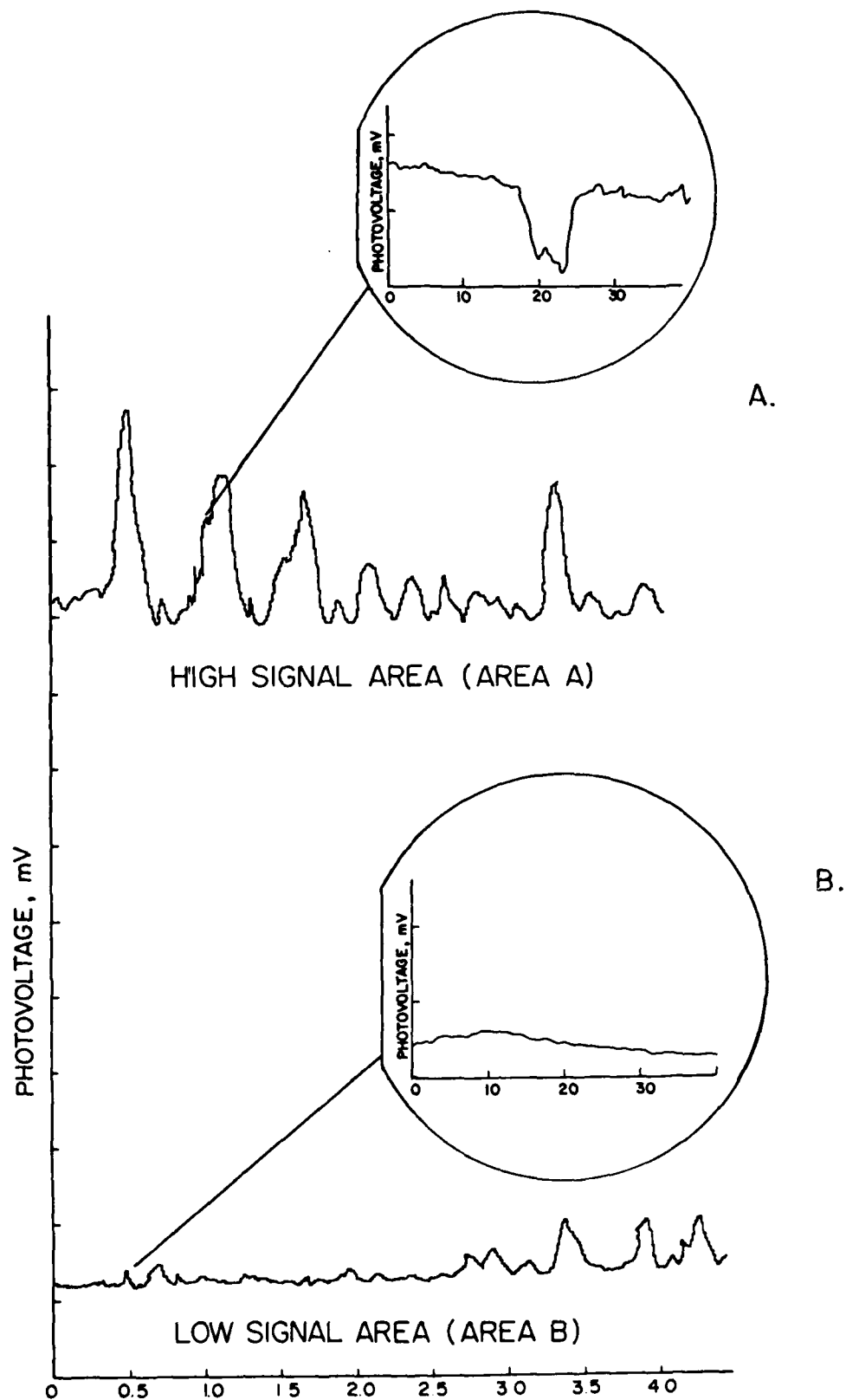


Figure 6. PV High-Resolution Profiles - As-Received GaAs Wafer.  
 (A) Area A - Figure 5; (B) Area B - Figure 5.

For comparison, we show on the right hand-side of Figure 5, the SPV responses obtained on the same wafer after some of the subsurface damage was removed by non-contact polishing (NCP) processing. In this case, the same wafer was mapped after NCP processing removal of about 50 microns of material from the surface. This processing removes most of the remnant traces of subsurface microstructural damage and internal deformation. We observe a significant reduction in the photovoltage extrema as well as in the spatial variations indicating that electrically-active defects have been removed along with the surface damage. It should be noted that some photovoltage activity is still observed in the highly defective zones, particularly near the wafer flat. Therefore, in this area, the NCP processing did not remove sufficient material to eliminate all the defects. These results illustrate that the SPV technique is useful in determining the extent of remnant defects and also could be used as a process monitor to determine polishing quality.

## 5.2 Resolution Measurements

5.2.1 Scribe-Induced Damage. To determine the resolution by direct damage profiling, SPV measurements were made on scribe damage introduced on a non-contact-polished (NCP)<sup>t</sup> LEC GaAs wafer. Scribing with a controlled-force (automated) scriber produced narrow, yet visible, near-one-micron damage traces. The near-surface remnant damage was removed before scribing because previous experiments had indicated that the propagation of scribe damage is minimized on an undamaged surface (to be discussed later). A high-resolution

---

<sup>t</sup>NCP processing is a controlled etching procedure implemented at ARACOR to remove remnant subsurface damage and deformation in semiconductor wafers (GaAs, InSb, CdTe, etc.). Previous results that demonstrate the improvement of surface quality by NCP processing have been described in reports and publications(7,8,9). These studies include evaluation of NCP surfaces by defect etching, RBS measurements, and measurements of improved device response on epitaxial layers and improved electrical performance in directly ion-implanted devices.

SPV trace of such a scribe line is shown in Figure 7. The damage trace has a measured mean width of about 2.5 microns. To correlate this SPV scan with direct wafer damage, a cross-section transmission electron micrograph was made to image the scribe-induced dislocations. These data are shown in Figure 8. Direct measurements on this micrograph indicate dislocations extending about three microns laterally. Some isolated dislocations are seen to extend about five microns into the bulk. Comparison between the SPV and TEM damage measurements indicates good agreement in the lateral damage profile; these data are consistent with a laser-spot-limited resolution of about 1.5 microns.

Preliminary experiments indicated that the presence of deep subsurface damage in conventional wafers enhances the lateral propagation of scribing-induced defects and, thus, results in die loss during the dicing step in GaAs wafers. In addition, it has been shown that lateral damage propagation during scribing can be essentially eliminated on NCP-processed wafers. SPV responses were found to accurately characterize the damage introduced by scribing.

GaAs wafers were diamond scribed using various loads followed by examination by optical microscopy, SEM and TEM. In wafers where scribing pressure was optimized (force ratios = 1.0, 1.5, and 2.0), visual damage was limited to deep traces of about 1.5 microns with light slip damage surrounding this line. When a damage delineation etch was used on these wafers, clearly defined lateral subsurface damage, extending beyond the optically-visible deep damage, was observed. These results are indicated in the attached micrographs (Figure 9 and Figure 10).

To determine the influence of remnant subsurface damage on the propagation of lateral scribing damage, standard and NCP wafers were subjected to scribing with an optimized load pressure. The delineation of these wafers with a defect delineation etch indicated that the lateral damage propagation was significantly reduced in the NCP wafers (Figure 10).

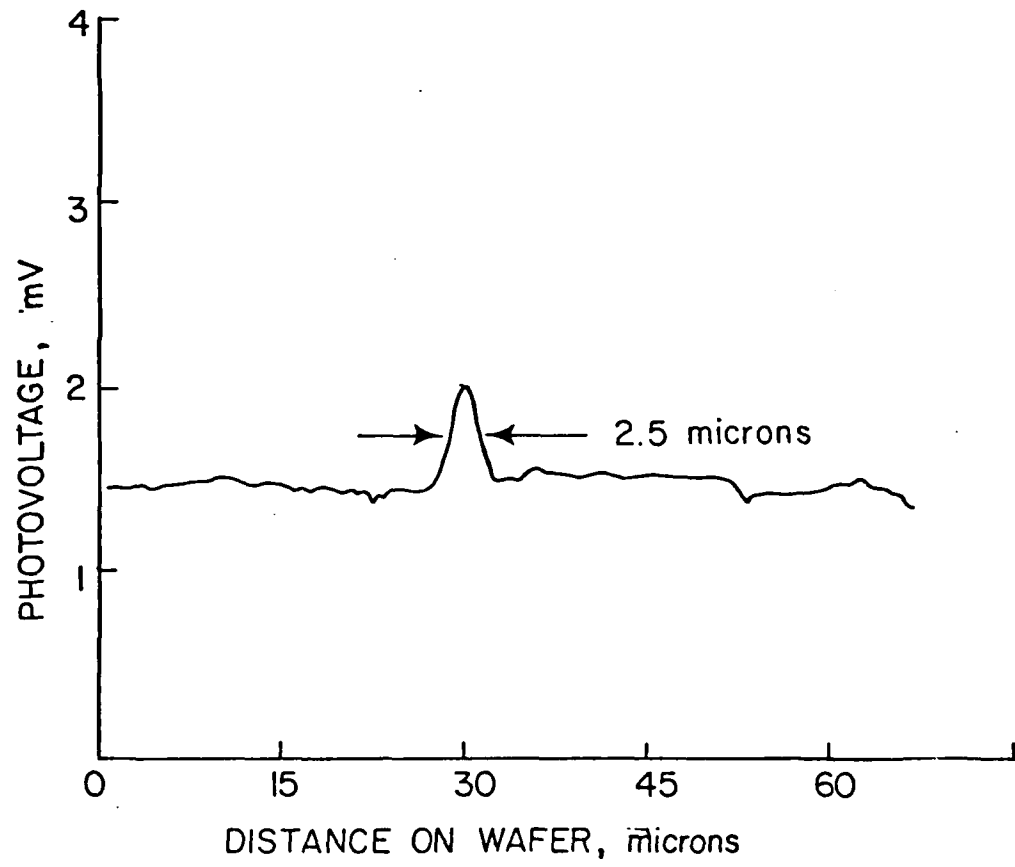


Figure 7. PV Profile of Scribe Damage on NCP GaAs Wafer. Minimum Force Was Used in Scribing Line. TEM in Figure 8 Shows Damage Corresponding to this Trace.

## CROSS-SECTION TEM OF SCRIBE DAMAGE

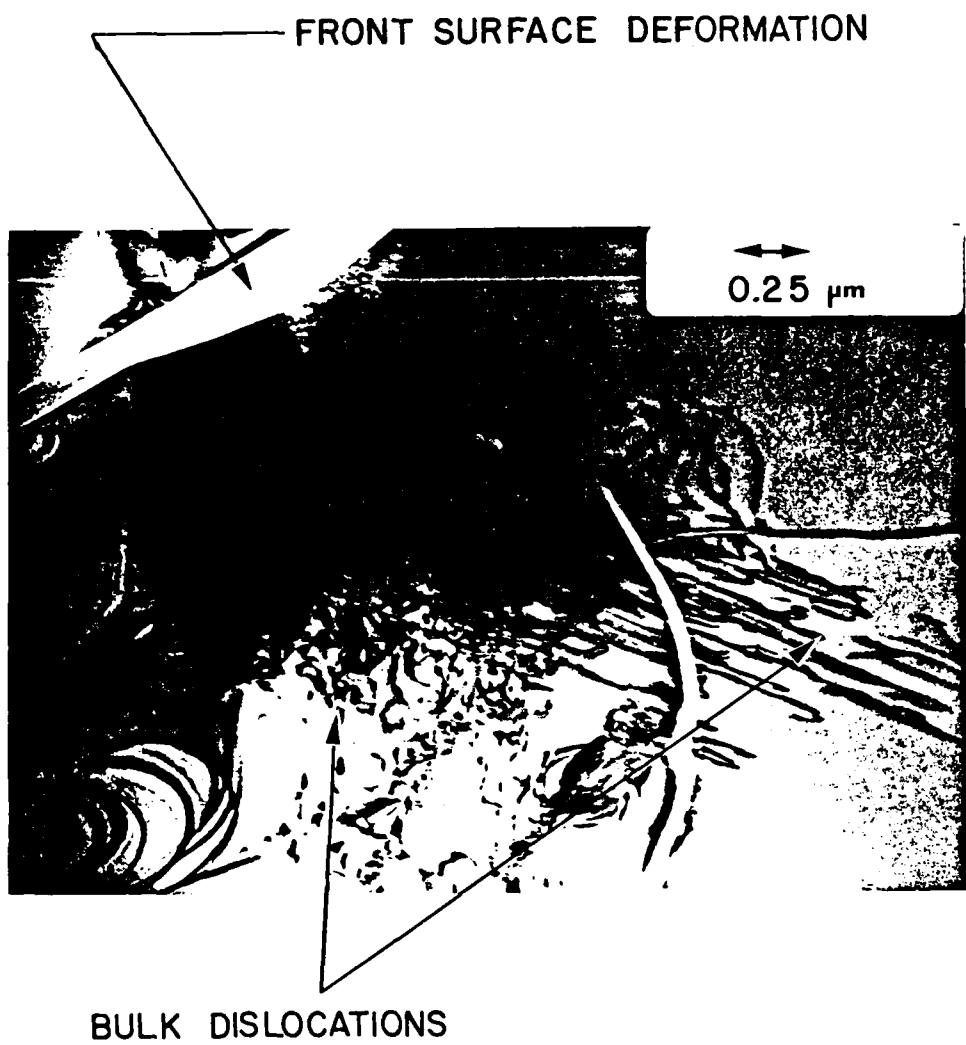
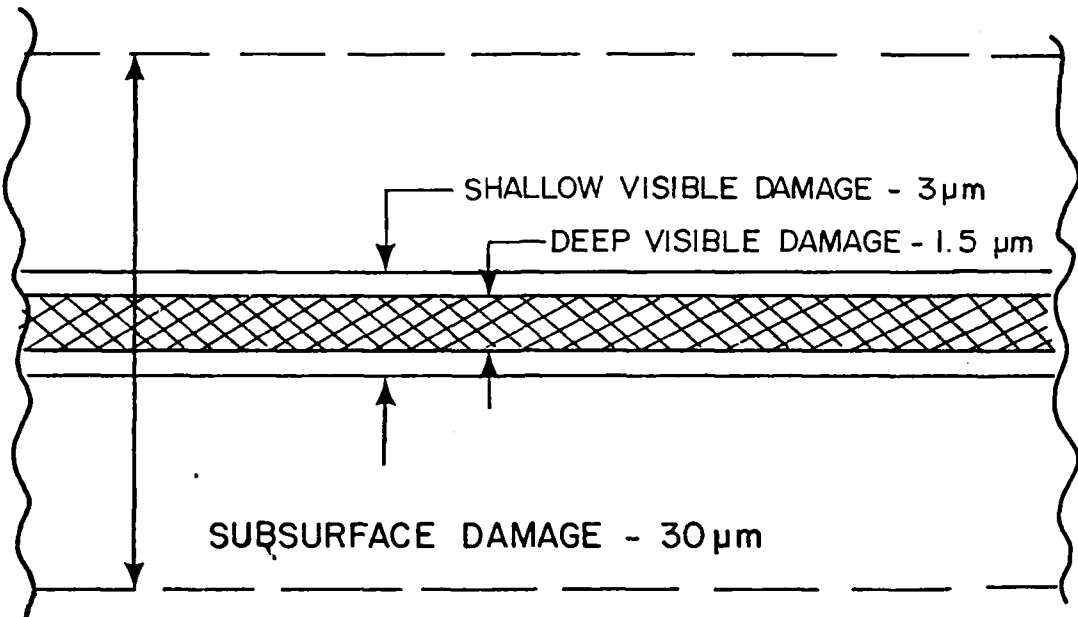
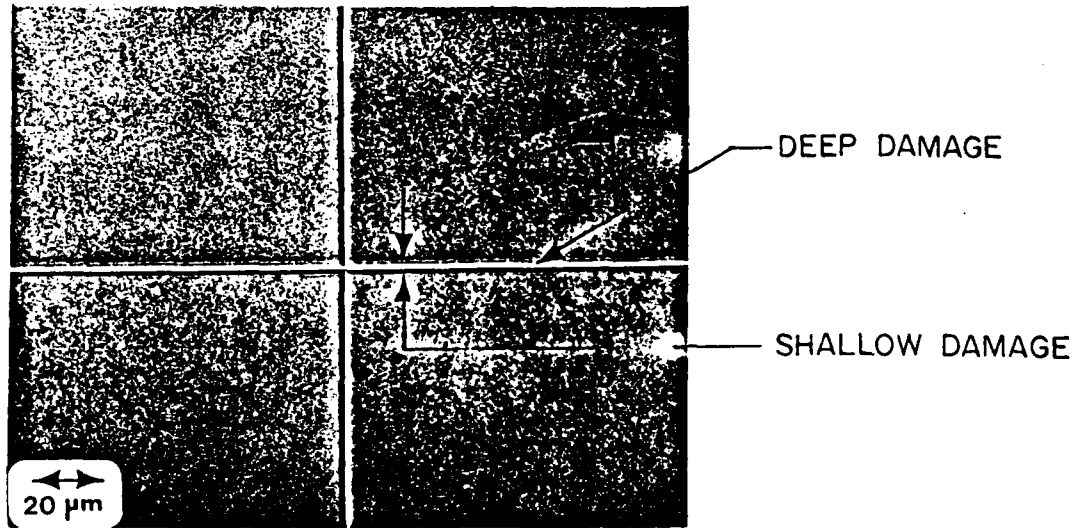


Figure 8. TEM Cross-Section of Scribe Damage for Same Wafer Used in Figure 7.  
The Lateral Extent of Dislocations Produced by Wafer Scribing are Shown.

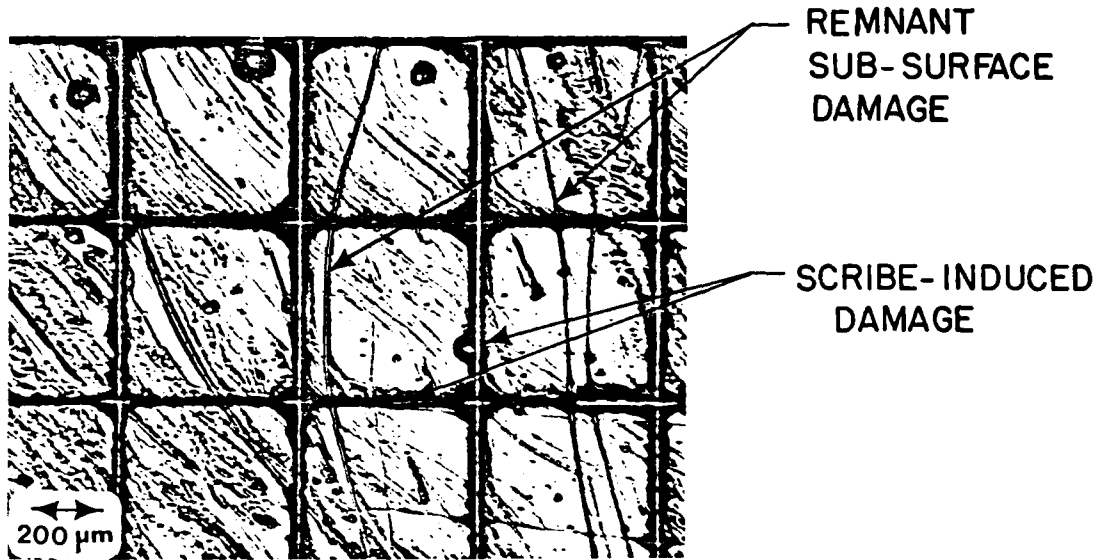


a) Schematic

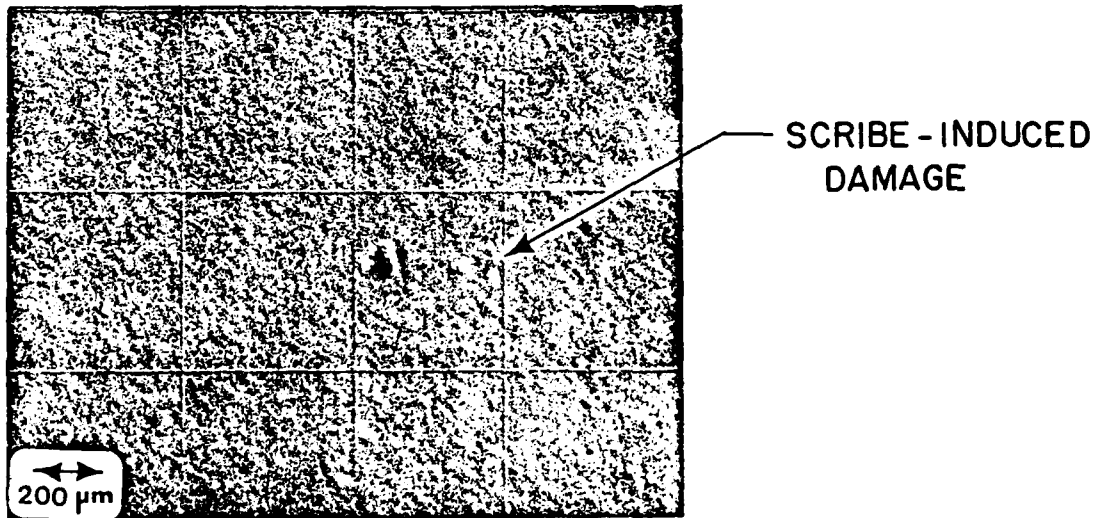


b) Micrograph

Figure 9. Scribe-Induced Damage



A. as received



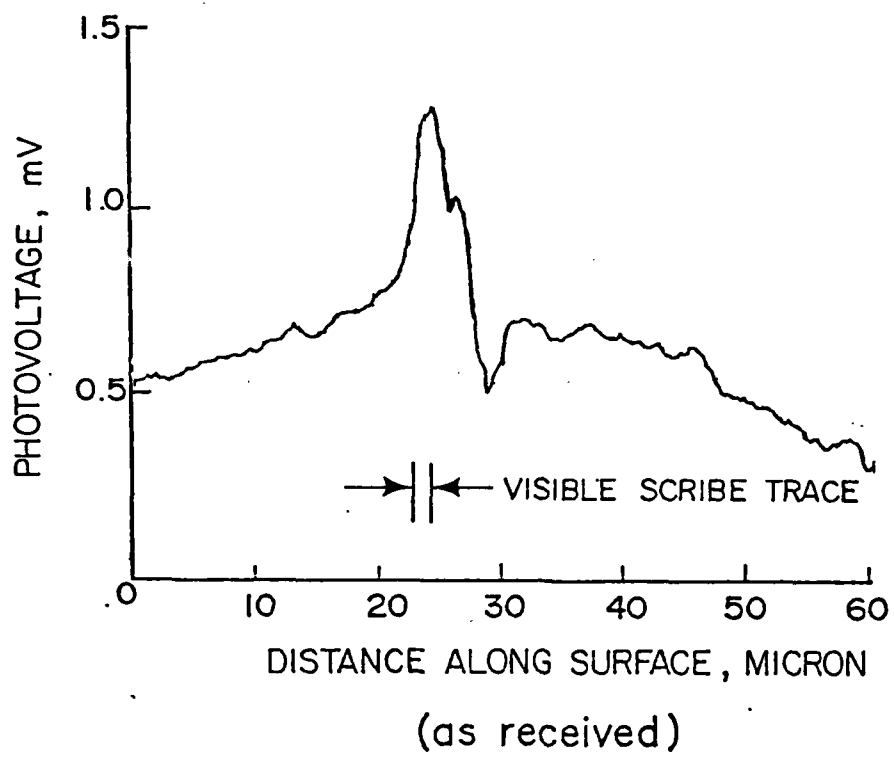
B. ncp

Figure 10. Scribe-Induced Damage - Lateral Spreading of Defects.  
(A) As Received; (B) NCP

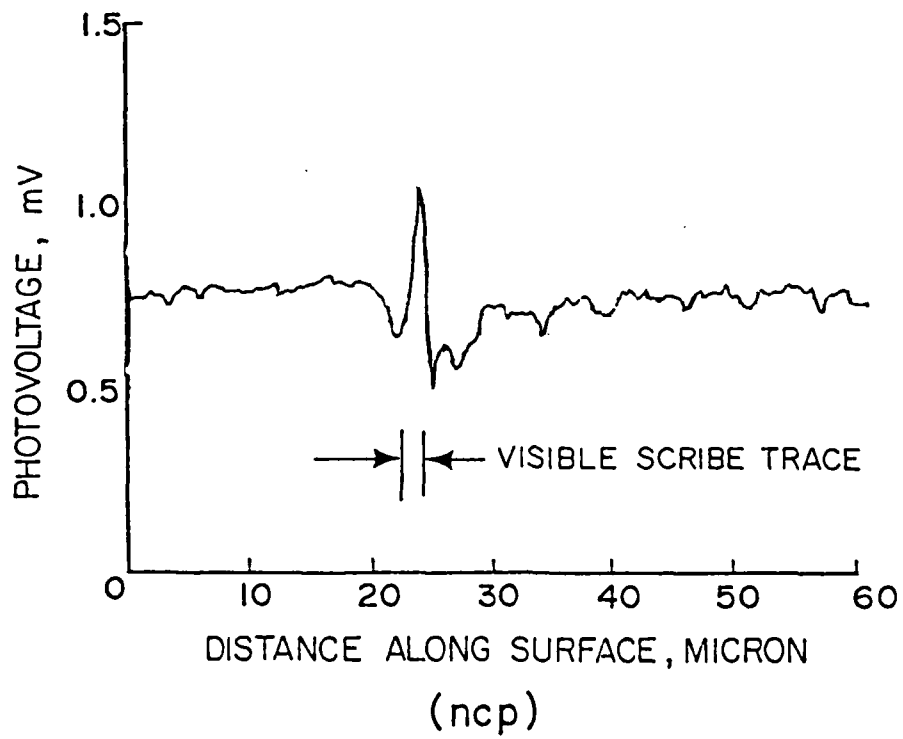
To clarify the extent of electrically-active defects as compared to defects delineated by etching, high-resolution SPV scans were made on these surfaces. The SPV responses (Figure 11) indicate that the extent of electrically-active subsurface damage induced by scribing is about 15 to 20 microns on standard wafers. Similar data indicate that this damage is confined to a region of about five microns on the NCP wafers.

The delineation etching shown in Figure 10 indicates spatial variation in the scribe damage, perhaps due to local flatness variations in the wafer surface. Similar variations were also observed in the SPV scans of electrically-active defects. In Figure 12, damage traces displaced by 15 microns are shown. Note the variations in both the scribe and background damage on this as-received wafer. The influence of variations in scribe forces is shown in Figure 13. Increases in both SPV peak and lateral responses are observed. These data suggest that the SPV response is sensitive to both the magnitude and lateral extent of surface damage and also suggest the quantitative correlation between SPV response peak height and surface damage.

**5.2.2 Effect of Orientation of Damage Traces.** To further illustrate the dependence on spatial positioning of damage traces, PV profiles were obtained perpendicular and parallel to damage traces in the substrate. Figure 14 shows the results of these measurements. In the perpendicular line scan, the extrema are periodic and the overall trend matches the damage concentration across the lineated substrate damage traces. When the scan is parallel to lineated damage in regions of low substrate density, the magnitude of the PV signal and the periodic nature of the trace are absent. Hence, it is now clear that the spatially-variable, electrically-active regions in the SOS film are correlated with the pattern of development of substrate damage.



(as received)



(ncp)

Figure 11. PV High-Resolution Profile Revealing Electrically-Active Defects Introduced by Scribing. (A) As Received; (B) NCP

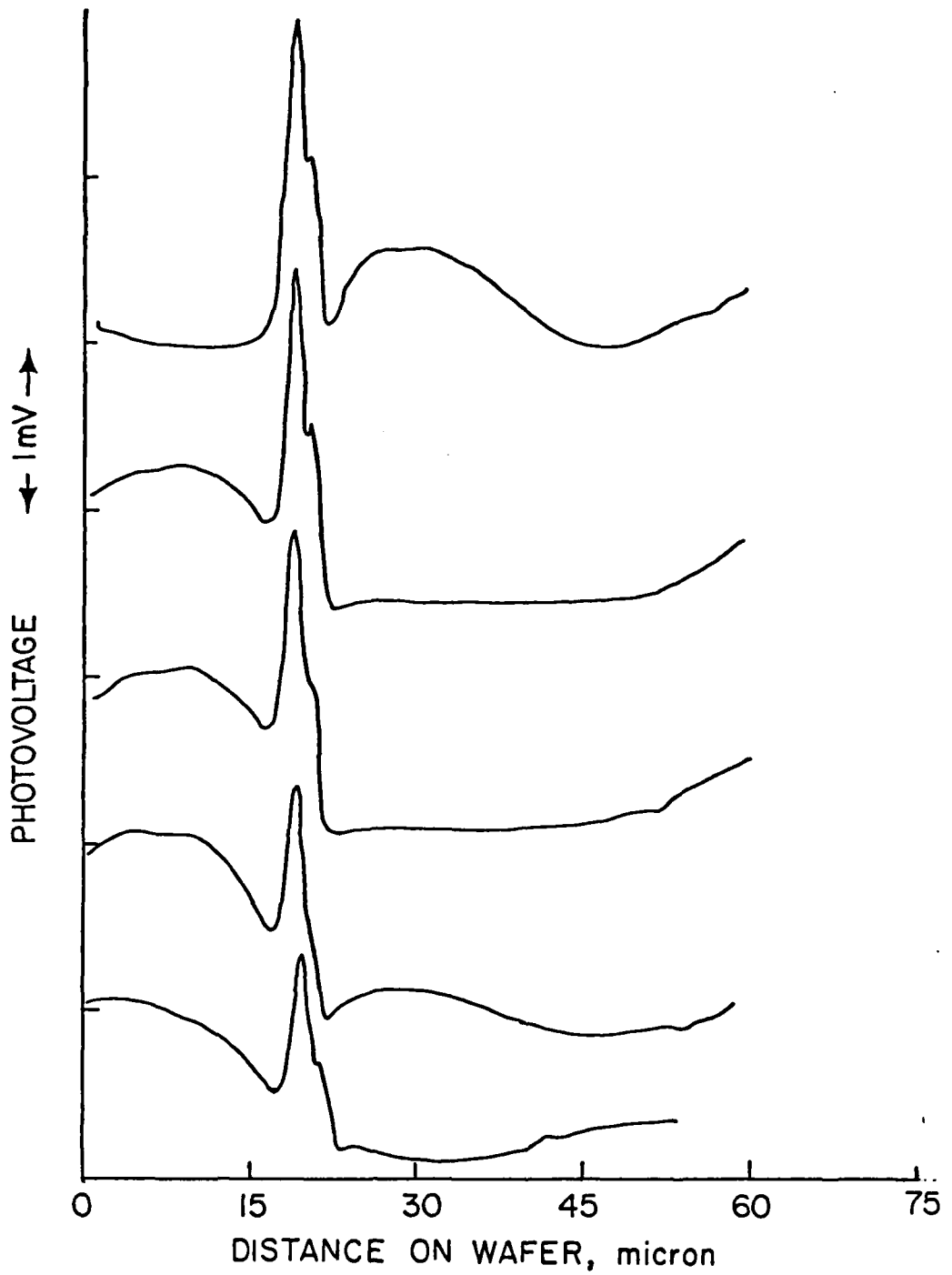


Figure 12. PV High-Resolution Profile Along Scribe - Curves Shown are Offset by 15 Microns - As-Received GaAs Wafer.

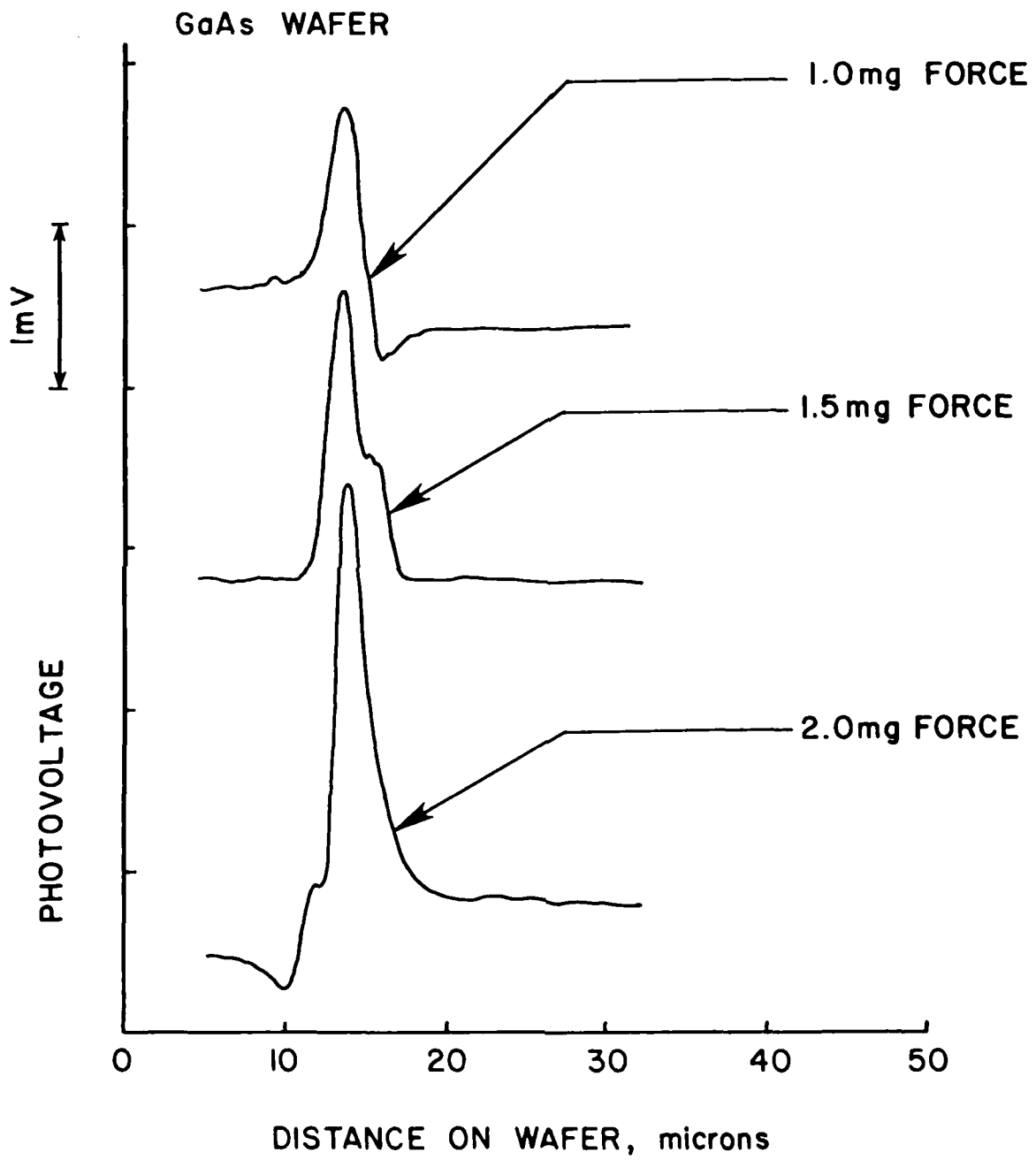


Figure 13. PV High-Resolution Profiles for Different Scribe Forces.

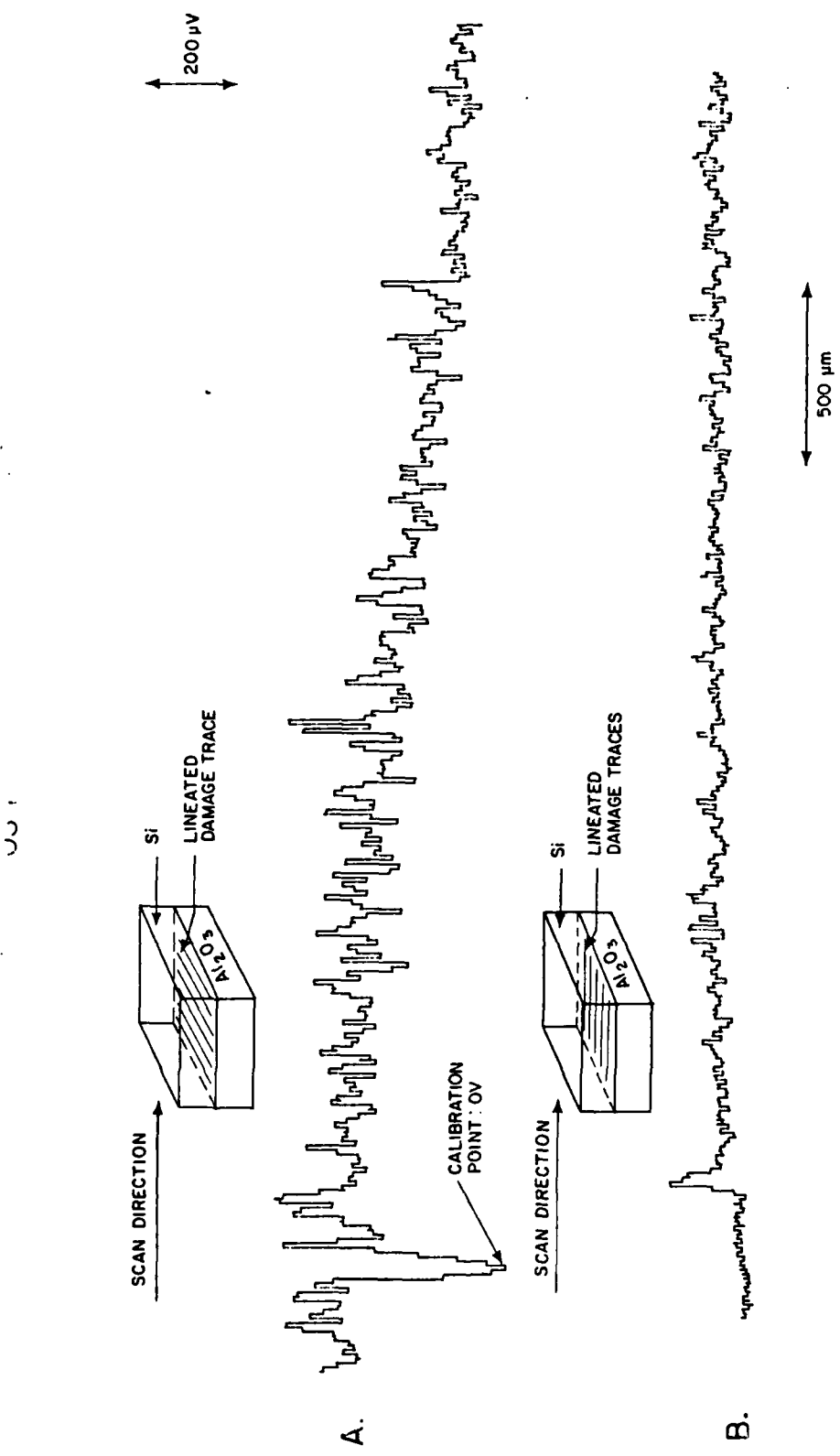


Figure 14. PV Profiles From SOS Film. (A) Scan Perpendicular to Lineated Damage; (B) Scan Parallel to Lineated Damage

### **5.3 GaAs - Effect of Non-Contact Polishing (NCP)**

Another application of the technique has been to the study of the surfaces of semiinsulating GaAs. In particular, we have investigated the effect on the photovoltage response of a non-contact polishing step(7,8,9). Figure 15 shows a SPV scan through the center of a 2-inch GaAs wafer as received from a commercial supplier. Figure 16 shows a high-resolution SPV scan on the as-received wafer indicating damage with spatial features ranging from 5-to-50 microns. It is known from prior work that lineated damage from incomplete polishing has spatial peaks located at 25-to-50 micron intervals. Figure 17 shows an SPV scan on the GaAs wafer after non-contact polishing (NCP). The reduction in the differential photovoltage signal is apparent for the wafer that received the NCP step as compared to the conventionally-polished wafer. This experimental finding is in agreement with prior experiments at ARACOR with NCP(7,8). Other characterizations of these substrates, including defect etching and TEM indicated that the smoother photovoltage response is directly correlated with decreased surface damage in the substrate.

The SPV scans shown are produced with a laser intensity of about 5 mW modulated at 15 Hz. The photovoltage is amplified by an electrometer-input preamplifier and detected by a lock-in amplifier set to integrate for 0.3 seconds. Therefore, the high-resolution scans are produced at a scan rate of about 180 microns/minute. Increasing the x-y step size produces whole-wafer scans (3 cm) in about two minutes.

### **5.4 SOS Films**

The PV response from SOS films grown on Kyocera and Union Carbide substrates are shown in Figure 18 and Figure 19. Additionally, Figure 20 shows a so-called "fast scan" of an SOS film grown on a Union Carbide substrate. This mode can provide rapid defect characterization over large areas.

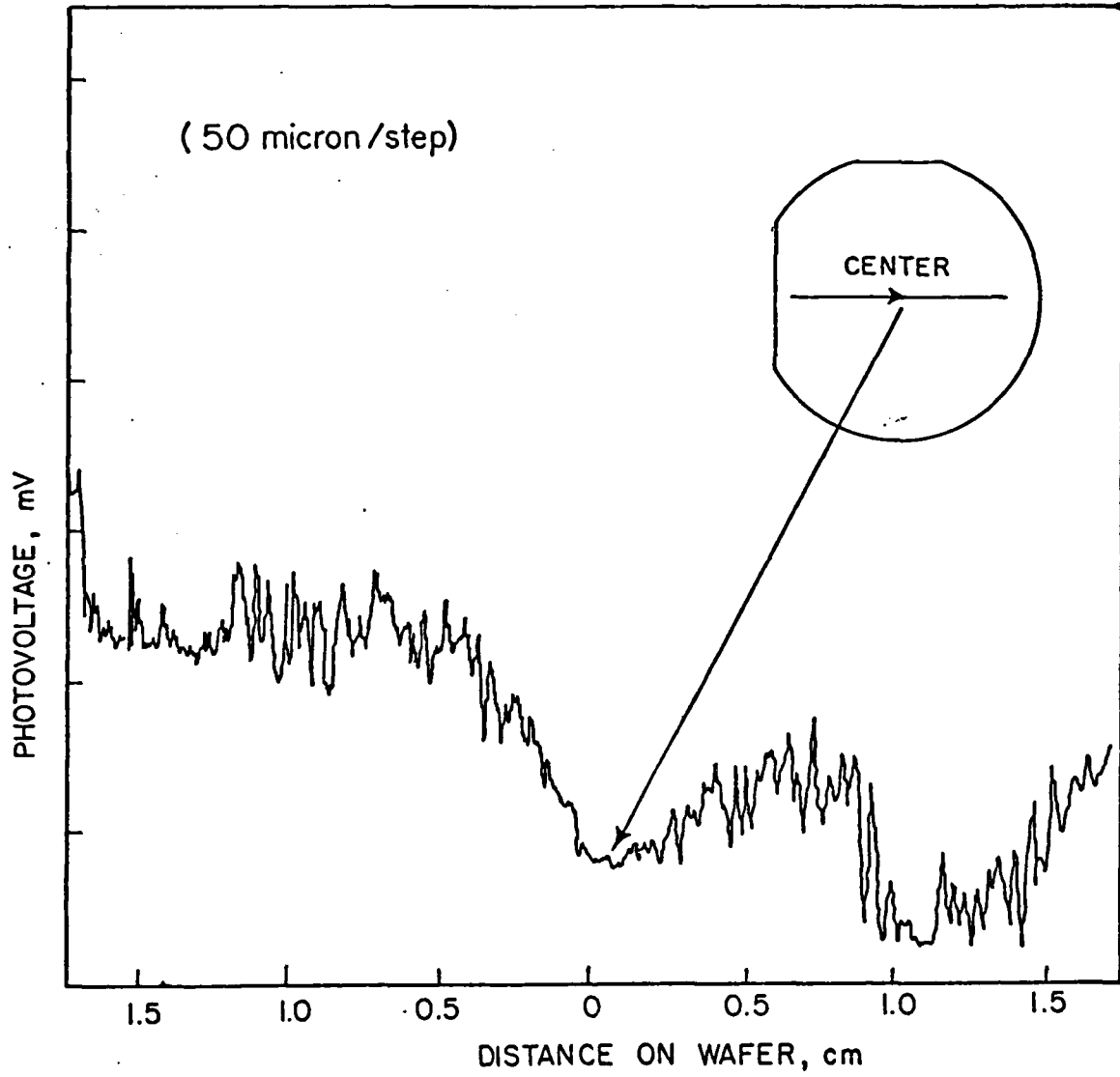


Figure 15. PV Profile - As-Received GaAs Wafer.

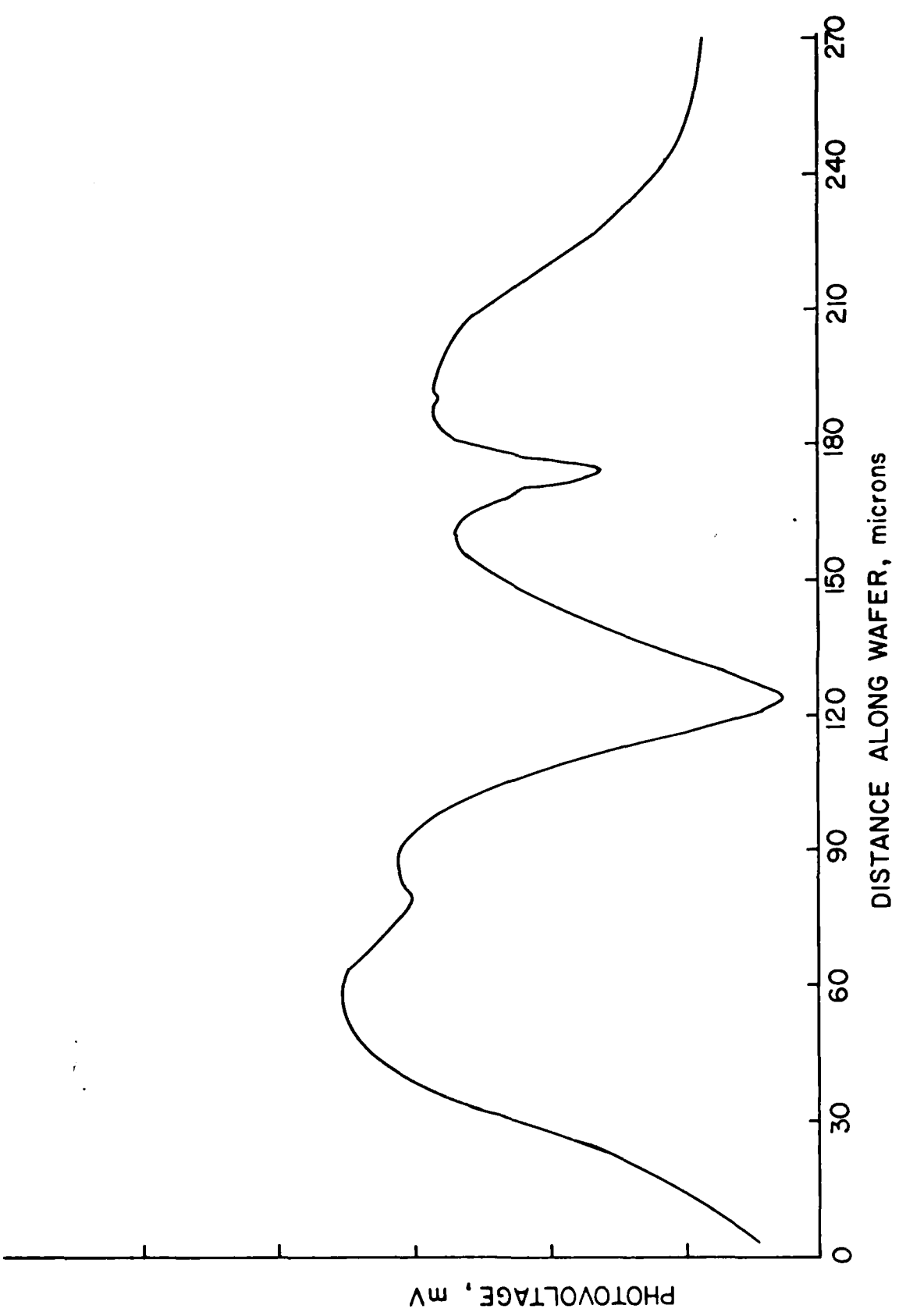


Figure 16. PV High-Resolution Profile - As Received GaAs Wafer.

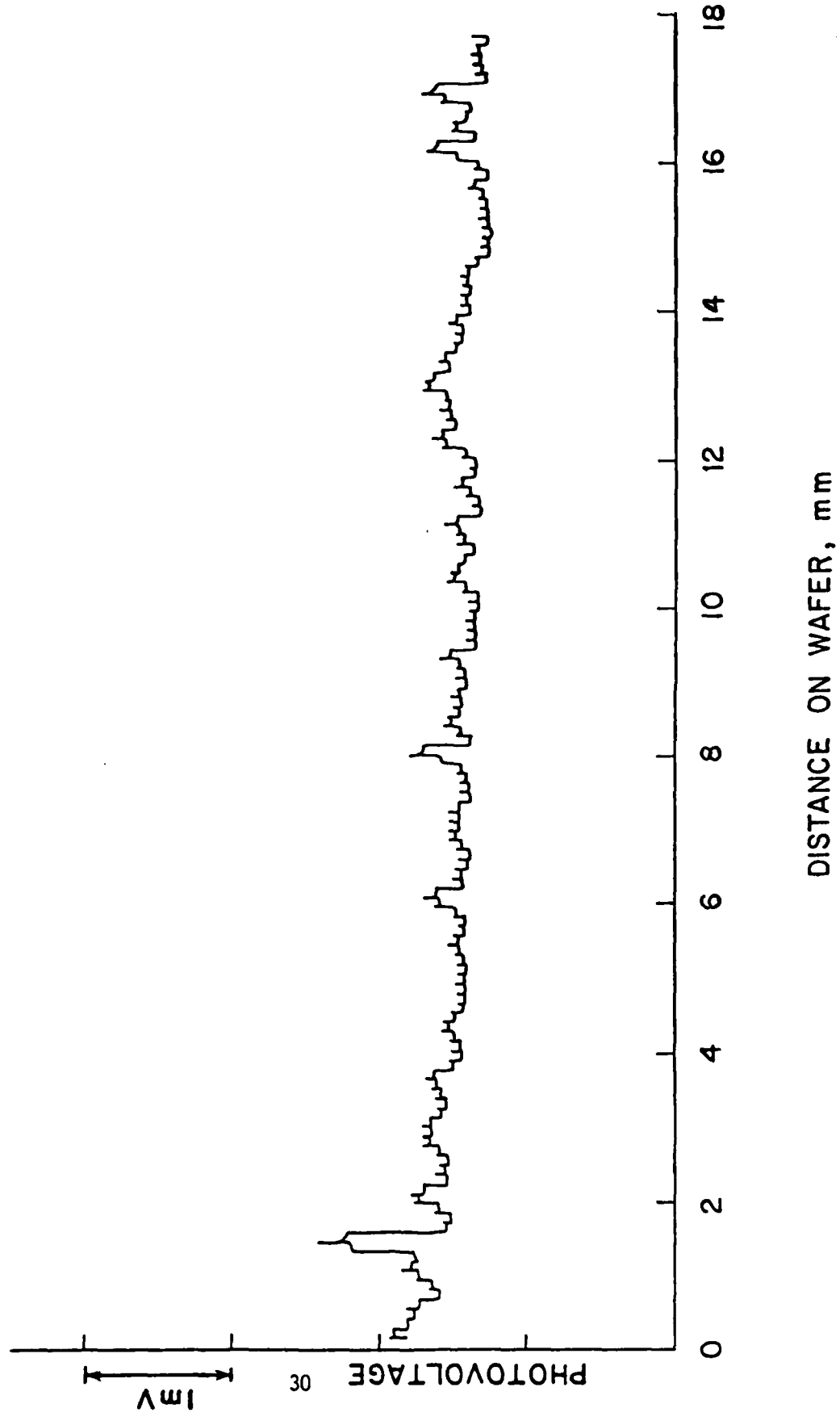


Figure 17. PV Profile After NCP Processing - GaAs Wafer.

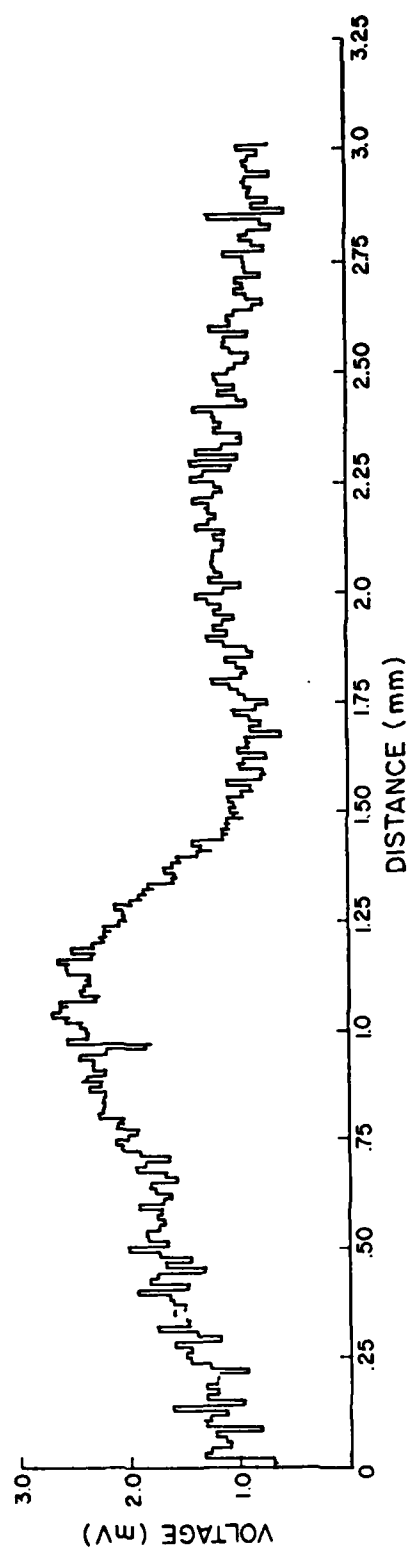


Figure 18. PV Profiles From SOS Film - Kyocera Sapphire.

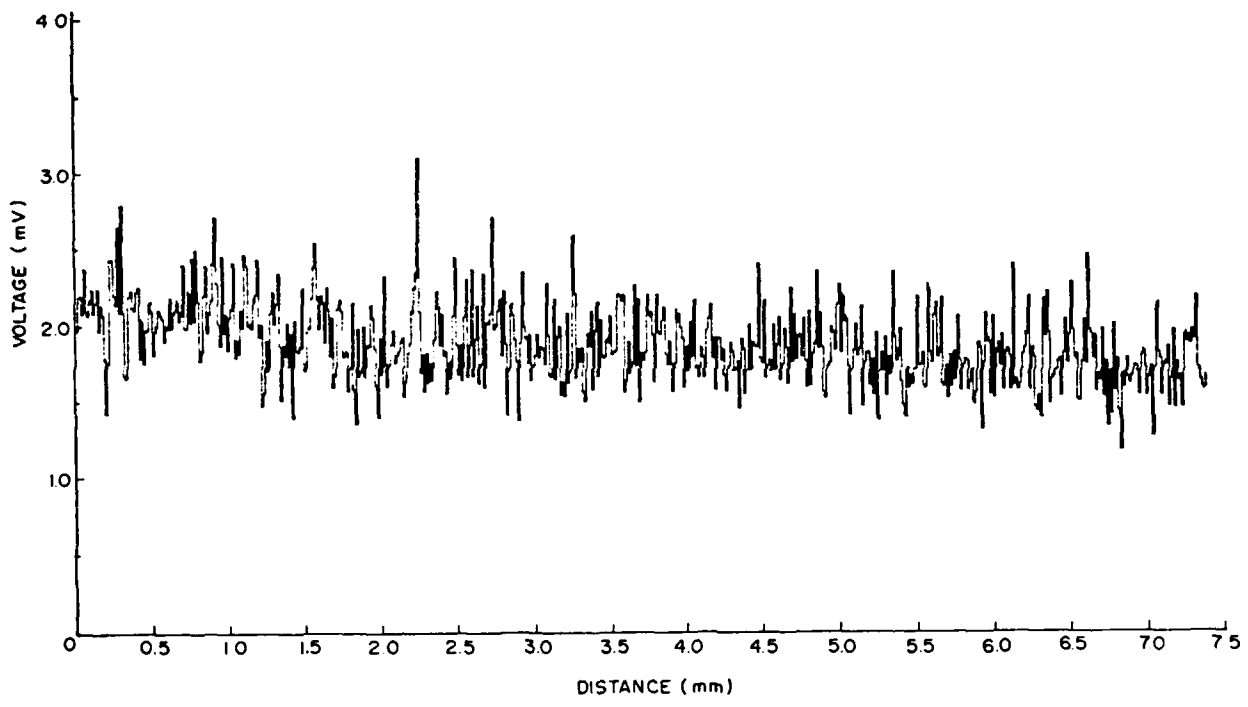


Figure 19. PV Profile From SOS Film - Union Carbide Sapphire.

PV RESPONSE-SOS FILM (UNION CARBIDE)

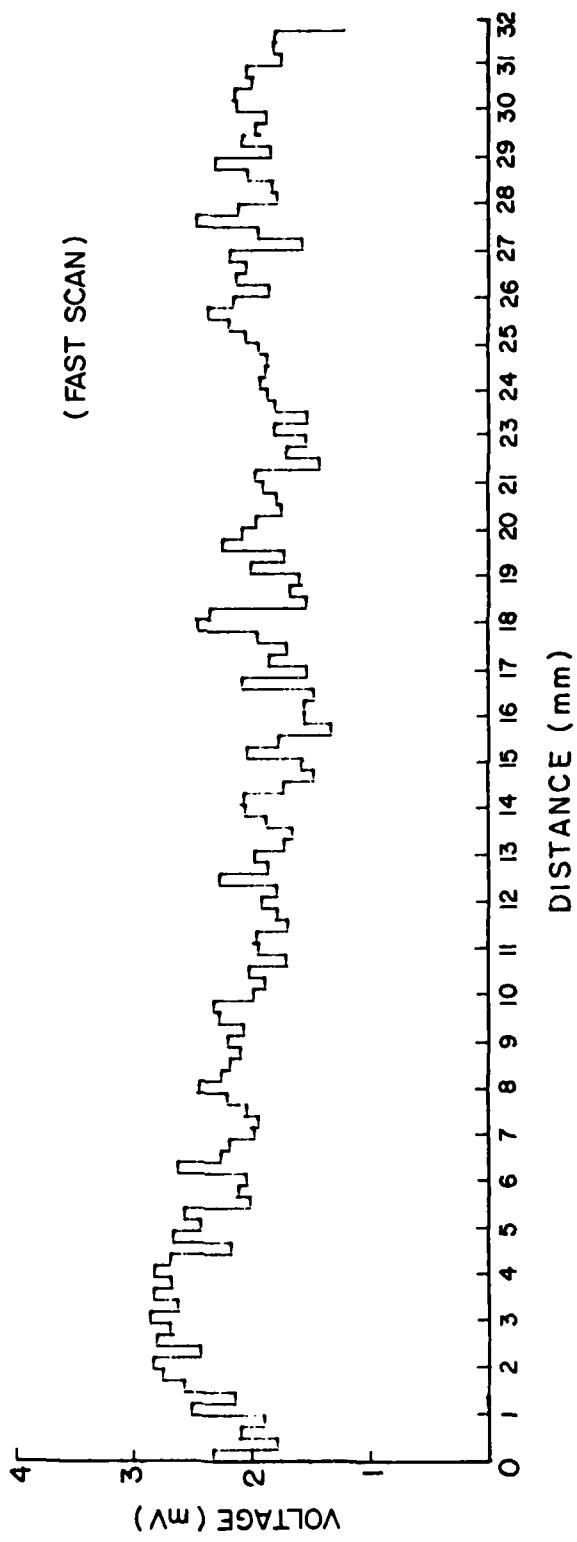


Figure 20. PV Profile From SOS Film Using Fast Scan - Union Carbide Sapphire.

## 6.0 SUMMARY AND CONCLUSIONS

This program focussed on evaluating the potential of the scanning photovoltaic technique for measuring the quality of semiconductor surfaces. Measurements were made of the SPV resolution and SPV signals were correlated with optical and electron microscopic measurements of defects. A summary of the principal results is provided below.

- The SPV technique is a non-destructive tool if incorporated with non-sintered contacts.
- Non-sintered contacts yield essentially the same signal as sintered contacts.
- Differential SPV signal is correlated with remnant polishing/handling damage in GaAs and can resolve near-surface defects.
- Resolution is determined by beam optics and carrier diffusion length to approximately 1 micron.
- The SPV technique is applicable for whole wafer evaluation.
- The SPV technique is insensitive to sample deformation effects that limit other techniques (RBS, x-ray, etc.).

The SPV instrument as described in this report can be developed into a commercially-viable tool for assessing the residual microstructural defect damage in GaAs wafers, as well as surface dislocations. The results indicate that the SPV technique could be used for incoming wafer inspection, as a process monitor to determine polishing quality and in device physics experiments for correlating wafer surface properties with device yield, performance and radiation hardness.

## 7.0 RECOMMENDATIONS FOR FUTURE WORK

- Automated data acquisition and digital signal processing of the SPV signal should be used to produce wafer maps. Work initiated in Phase I to provide some digital control should be completed.
- Optimize SPV signal to increase the detection sensitivity, resolution and throughput rate.
- Extend multi-wavelength operation in order to simultaneously resolve surface and bulk defects and minimize spurious signals.
- Improve the contacting scheme in order to minimize the wafer contact needed to produce reliable SPV responses. Work on producing backside-illuminated contacts is proposed. Methods utilizing electrolytes to contact the surfaces and provide low resistance contacts will be investigated. The process must be optimized to minimize wafer contamination.
- Employ the SPV technique for mapping and characterizing commercial GaAs wafers.
- Correlate SPV signals with electrical measurements made on test structures on GaAs wafers. In this manner, the influence of process-induced defects and surface mobility variations can be determined.
- Perform cross-correlation experiments using SPV scanning, optical microscopy with delineation etching, planar and cross-section TEM, EBIC measurements, X-ray topography, minority carrier lifetime, Rutherford backscattering, and thermal-wave microscopy. The purpose of these experiments is to establish figures of merit for the PV defect maps.

## 8.0 REFERENCES

1. H. J. Leamy, L. C. Kimerling, and S. D. Ferris, "Scanning Electron Microscopy," 1978, Vol. 1, SEM Inc., AMF O'Hare, IL 60666, 717.
2. J. Oroshnik and A. Many, J.E.C.S., 106, 360 (1959).
3. J. Lagowski, L. Jastrzebski, and G. W. Cullen, J.E.C.S., 128, 2665 (1981).
4. L. Jastrzebski, J. Lagowski, G. W. Cullen and J. I. Pankove, Appl. Phys. Lett., 40, 713 (1982).
5. J. Lagowski, L. Jastrzebski, and G. W. Cullen, J.E.C.S., 129, 2609 (1982).
6. T. I. Chappell, P. W. Chye, and M. A. Tavel, Solid State Electron, 26, 33 (1983).
7. T. J. Magee and R. D. Ormond, "Hydroplane Polishing of CdTe Wafers," Informal DARPA Report of Significant Accomplishment (February 1982).
8. T. J. Magee and P. M. Raccah, "Improvement in CdTe Surface Structure and LPE-HgCdTe Layer Quality Using Non-Contact Substrate Polishing," Proceedings of IRIS, (July 1982).

END

FILMED

5-86

DTIC